THIS BOOK IS OF POOR LEGIBILITY DUE TO LIGHT PRINTING THROUGH OUT IT'S ENTIRETY.

THIS IS AS RECEIVED FROM THE CUSTOMER.

ULTRASONIC ABSORPTION BY METAL CHELATES

by

JEFFREY BARTNER

B. S. College of Emporia, 1973

A MASTER'S THESIS

submitted in partial fulfillment of the

requirements for the degree

MASTER OF SCIENCE

Department of Chemistry

KANSAS STATE UNIVERSITY
Manhattan, Kansas

1976

Approved by:

Clifton E. Melson
Major Professor

ACKNOWLEDGMENTS

The author wishes to thank Don Rempel for his assistance in some of the instrument design. Much time was spent by Mr. Rempel which is indicative of his commitment to the field of electronics.

The author also wishes to acknowledge his major professor, Dr. Clifton E. Meloan who provided the encouragement and guidance while the author developed his own skills.

The author's research group is acknowledged for providing the wit and wisdom, both of which have become an integral part of this project.

This work would not have been possible without the love, understanding and sacrifice of the author's wife, Cathy, who has done more for its completion than she will ever know.

The National Science Foundation is gratefully acknowledged for its financial support in the form of research assistantships.

TABLE OF CONTENTS

LIST OF TABLES

LIST OF FIGURES

Introduction

Previous work in this research group on the mechanism of the liquid-liquid extraction of metal chelates has shown that many metal chelates have both water and organic solvent molecules as an integral part of the extracted species (1-7). Two fundamental questions that are asked here are 1) How fast do these adducts exchange and 2) What is the overall activation energy? The work by Ford (8) of this group showed that an ultrasonic pulse could possibly be used to obtain this information.

The research reported here is based on building an instrument that is 10 times more sensitive than Ford's, that has a frequency limit above 100 MHz, and shows that overall reaction rates and activation energies can be obtained. In addition, proposals are made for further instrument improvements that hopefully will lead to the determination of the stepwise rate constants and energies.

The equipment used in this research was basically that of Ford's but almost every device has either been replaced or optimized. The signal generator used previously employed a Wien bridge oscillator. The wave form of this was not constant and would collapse after a period of time. This was replaced by a single integrated timing circuit. The double pulse generator still uses 3 discrete monostable multivibrators. However, they have been modified to improve wave form and pulse width accuracy. The entire pulse generator was converted

from several individual 25 volt power supplies to a single 5 volt logic supply.

Two major short comings of the instrument used by Ford were 1) it required a separate calibrated oscillator frequency for each frequency studied and 2) both signals were recombined through an impedance matching device that destructively coupled. The solution to both these problems was to multiplex both sample and reference pulses on one line. The variable frequency power oscillator was then converted to include both a high voltage and a low voltage output thus serving as both a sample and reference source. The receiver in turn would then select one or the other at the same rate the signals are multiplexed and at a rate which makes them appear coincident on the oscilloscope. The receiver itself has been completely rebuilt to increase both its range and sensitivity. This eliminated the need for the tuned amplifiers which previously were so cumbersome.

The Ultrasonic Method

It was believed that an ultrasonic pulse could be used to measure the kinetics of various metal chelates. Ultrasonics is particularly convenient for this, since an equilibrium reaction is all that is needed. We can therefore use the "Ultra-sound" waves to perturb the equilibrium of the system, then allow it to return to its initial state. The frequency of the ultrasonic wave that is absorbed depends on the mass of the absorbing species. The basic idea is to find a frequency that will break up the species and then monitor how

it reforms. The instrument discussed in this thesis is capable of measuring this overall effect.

Each system that one might study has its characteristic relaxation time, τ. If a system is a simple one step reaction, then only one value for τ would occur. For a more complicated multi-step process, a whole spectrum of τ's would result.

As an example, assume the equilibrium described by Caldin (9):

$$1) \quad A + B \underset{k_b}{\overset{k_f}{\rightleftharpoons}} C$$

Let a^*, b^* and c^* equal the equilibrium concentration and a, b and c to be the actual analytical concentration at any time, t. Then $\bar{a}$, $\bar{b}$, and $\bar{c}$ will be the time dependent equilibrium concentration during perturbation such that a^*, b^* and c^* will equal $\bar{a}$, $\bar{b}$ and $\bar{c}$ at the initial and final equilibrium.

Let us now define y as the difference at time t between the actual value (a, b and c) and the equilibrium values a^*, b^* and c^*; and $\bar{y}$ as the difference at time t between the time dependent equilibrium values $\bar{a}$, $\bar{b}$, and $\bar{c}$ and the equilibrium concentrations a*, b* and c*. This leads to:

$$2) \quad y = a - a^* = b - b^* = c^* - c$$

$$3) \quad \bar{y} = \bar{a} - a^* = \bar{b} - b^* = c^* - \bar{c}$$

or in terms of the time dependent variable:

$$4) \quad a = y + a^* \qquad \bar{a} = \bar{y} + a^*$$

$$5) \quad b = y + b^* \qquad \bar{b} = \bar{y} + b^*$$

$$6) \quad c - c^* - y \qquad \bar{c} = c^* - \bar{y}$$

The net forward rate expression for equation 1 is;

$$7) \quad \frac{-dy}{dt} = k_f [a] [b] - k_b [c]$$

$$8) \quad \frac{-dy}{dt} = k_f [y + a^*] [y + b^*] - k_b [c^* - y]$$

At equilibrium the rate is zero, therefore the expression for this would yield:

$$9) \quad \frac{-dy}{dt} = o = k_f [\bar{y} + a^*] [\bar{y} + b^*] - k_b [c^* - \bar{y}]$$

Setting equation 8 equal to equation 9 we obtain:

$$10) \quad \frac{-dy}{dt} = k_f ([y + a^*] [y + b^*] - [\bar{y} + a^*] [\bar{y} + b^*])$$

$$-k_b ([c^* - y] - [c^* - \bar{y}])$$

$$= k_f ([\bar{y}^2 + a^*\bar{y} + b^*\bar{y} + a^*b^*])$$

$$-[\bar{y}^2 + a^*\bar{y} + b^*\bar{y} + a^*b^*])$$

$$-k_b (c^* - y - c^* + \bar{y})$$

$$= k_f (y^2 - \bar{y}^2 + a^*y + b^*y - a^*\bar{y} - b^*\bar{y})$$

$$-k_b (\bar{y} - y)$$

$$= k_f ([y^2 - \bar{y}^2] + y [a^* + b^*] - \bar{y} [a^* + b^*])$$

$$-k_b (\bar{y} - y)$$

$$= k_f (y^2 - \bar{y}^2 + [a^* + b^*] [y - \bar{y}]) - k_b$$

$$(\bar{y} - y)$$

$$11) \quad \frac{-dy}{dt} = k_f (y^2 - \bar{y}^2 + [a^* + b^*] [y - \bar{y}]) + k_b (y - \bar{y})$$

In practice, there will be very small perturbations of the equilibria, therefore the y value will be small and it is

possible to eliminate the y^2 and $\bar{y}^2$ terms. Equation 11 would then yield:

$$12) \quad \frac{-dy}{dt} = (y - \bar{y}) \left(k_f [a^* + b^*] + k_b\right)$$

Since,

$$13) \quad \frac{1}{\tau} = k_f (a^* + b^*) + k_b$$

it follows that,

$$14) \quad \bar{y} = y + \tau \left(\frac{dy}{dt}\right)$$

In equation 14, $\bar{y}$ becomes the forcing function. It is this value which is changed by some applied external force. In this case, the ultrasonic wave induces a slight pressure change which perturbs the equilibrium.

It is assumed that the ultrasonic wave is sinusoidal. This is a good assumption because the driving function of the ultrasonic transducer is an R. F. sine wave. This means the pressure will also vary in a sinusoidal manner.

Hence:

$$15) \quad \bar{y} = A \sin \omega t$$

Equation 14 will then become:

$$16) \quad \tau \left(\frac{dy}{dt}\right) + y = A \sin \omega t$$

Solving this equation for y;

$$17) \quad y = A \sin \omega t - \tau \left(\frac{dy}{dt}\right)$$

which upon solving the differential equation, yields the following:

$$18)\quad y = \frac{1}{1+\omega^2\tau^2} A \sin\omega t - \left(\frac{\omega\tau}{1+\omega^2\tau^2}\right) A \cos\omega t$$

The first term of equation 18 is a sine function and therefore the variation of y is in phase with the ultrasonic wave. The second term, however, is a cosine function and the variations of y are out of phase with the ultrasonic wave. It is this phase lag which is responsible for the absorption of the acoustical wave.

We will now define u as the amount of absorption per cycle, which is proportional to the coefficient of the second term in equation 18, hence,

$$19)\quad u \propto \frac{\omega\tau}{1+\omega^2\tau^2}$$

This absorption, which can be measured in terms of the attenuation of the ultrasonic wave, is related exponentially to the distance (X) traveled through the sample.

$$20)\quad I = I_o e^{-\alpha X}$$

where I_o is the intensity of the wave at the transmitting crystal, and I is the intensity at distance X. α is the absorption coefficient measured in units of absorption (decibels) per centimeter $(\frac{db}{cm})$. In its actual application, α will be multiplied by 2 to take into account both half cycles of each wave.

What is needed now is a way of relating α which we can readily measure to τ and frequency. Since

21) $f = \frac{\omega}{2\pi}$

and u is the absorption per wave, we can then relate f and u by;

22) $u = \alpha\lambda = \frac{\alpha C}{f} = \frac{2\pi\alpha}{\omega} C$

where C is equal to the velocity of the sound wave. Hence, if $\frac{\alpha}{f^2}$ is plotted versus log f, the relaxation time (τ) can be found. This plot fits the curve:

23) $\frac{\alpha}{f^2} = \frac{A}{1 + (f/f_c)^2} + B$

See Figure 1 (9).

The frequency at the inflection point, f_c, is then related to τ by:

24) $\tau = \frac{1}{2\pi f_c}$

A in Figure 1 refers to the sample where B refers to the background. The background is caused by any substance which the acoustic wave encounters between the transducers, other than the sample. In practice, B refers to the solvent of the system and the membrane separating the solvent and sample. The background for most pure solvents is relatively low. The bigger the difference between A and B, the easier it is to detect the relaxation time. The magnitudes of A and B depend directly on the type of cell arrangement used.

The cell used here is of the differential type (10).

THIS BOOK CONTAINS NUMEROUS PAGES THAT WERE BOUND WITHOUT PAGE NUMBERS.

THIS IS AS RECEIVED FROM CUSTOMER.

FIGURE 1

A plot of $\frac{\alpha}{f^2}$ versus log f

showing the relaxation frequency f_c.

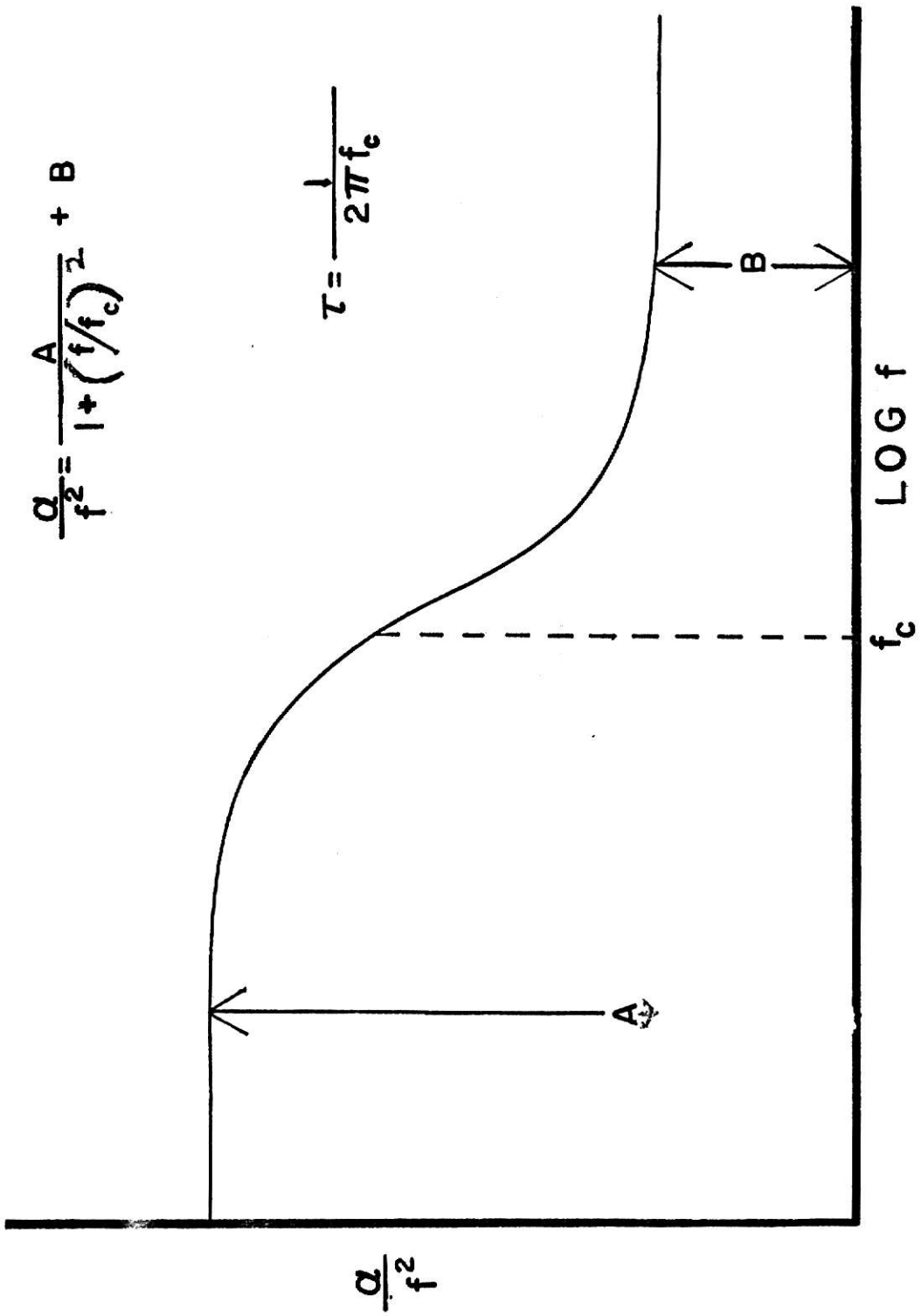
$\frac{\alpha}{f^2} = \frac{A}{1+(f/f_c)^2} + B$
$\tau = \frac{1}{2\pi f_c}$
B
A
f_c
LOG f
$\frac{\alpha}{f^2}$

This is shown in Figure 2. The cell is divided into two compartments, both of which are temperature controlled to within $\pm$ 0.1°C by means of a water jacket and an external constant temperature bath. The membrane which divides the two compartments is made of a material which is transparent to the ultrasonic waves. Acetate was used in this work but other materials such as Celanar and Mylar will work as well. One compartment contains the species under study dissolved in an appropriate solvent. The other compartment is filled with the solvent itself, which acts as the reference.

Recall that equation 20 related the ratio of the intensity, I, to α, the absorption coefficient and X, the distance the wave traveled through the sample. In practice there are three absorption coefficients of interest:

1) α_r which is due to the reference solution.

2) α_{sol} which is due to the solvent the species dissolved in and

3) α which is due to the species itself.

The value I_o is defined as the initial intensity of the ultrasonic wave at the transmitter, I_m as the intensity at the membrane and I as the intensity at the receiver.

Now consider an ultrasonic wave traveling from the transmitting transducers to the receiving transducer where it first passes through the dissolved species and then through the reference.

The intensity at the membrane is found by:

FIGURE 2

The schematic of the cell and crystal mount.

THIS BOOK CONTAINS NUMEROUS PAGES WITH DIAGRAMS THAT ARE CROOKED COMPARED TO THE REST OF THE INFORMATION ON THE PAGE.

THIS IS AS RECEIVED FROM CUSTOMER.

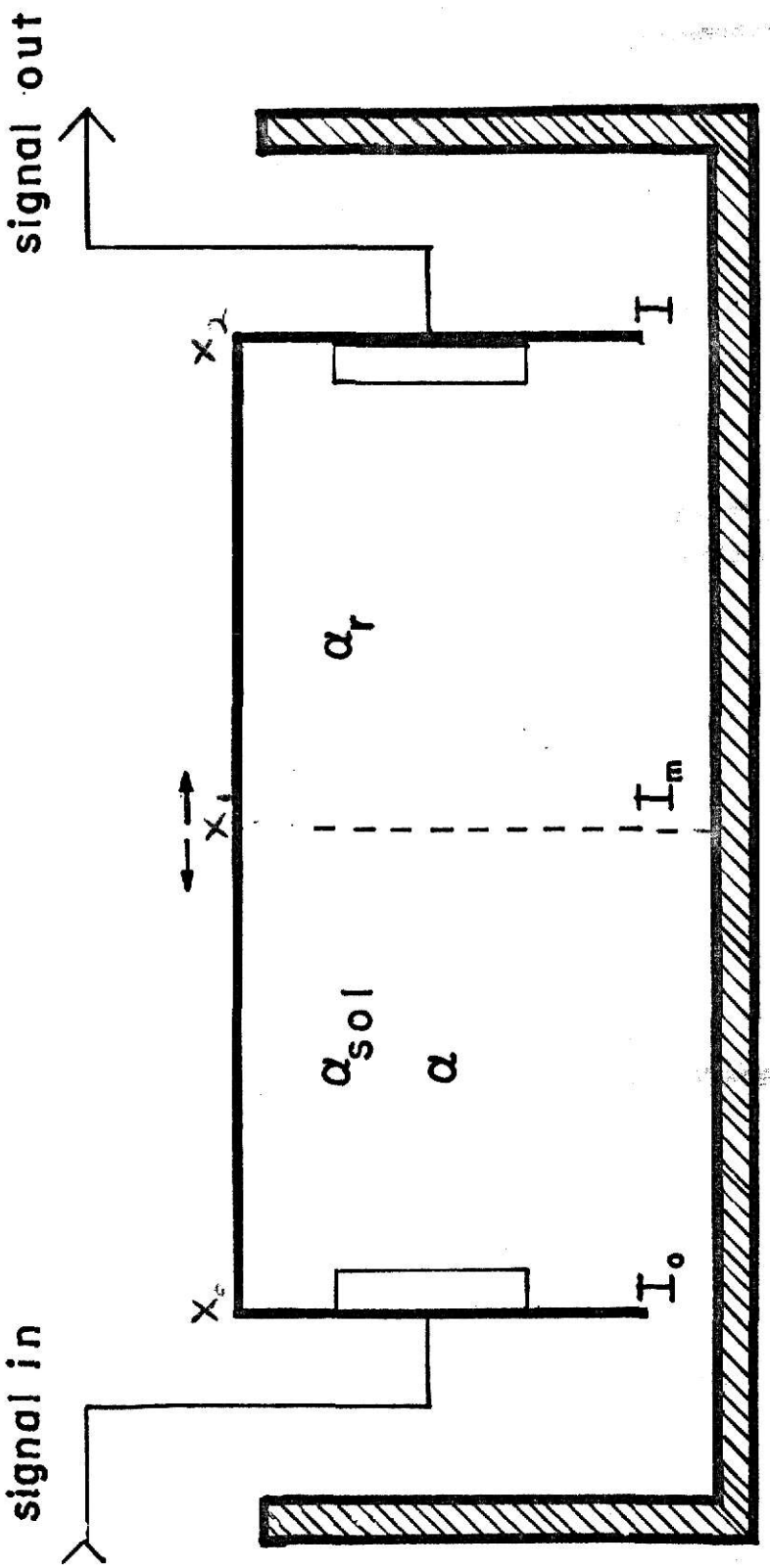
signal out
signal in
x_2
x_1
x_0
I
I_m
I_o
α_r
α_{sol}
α

$$25) \quad I_m = I_o \, e^{-2(\alpha + \alpha_{sol}) X_1}$$

The intensity at the receiver is found by:

$$26) \quad I = I_m \, e^{-2(\alpha_r)(X_2 - X_1)}$$

We can now combine equation 25 and equation 26 for an expression which describes the intensity throughout the entire system.

$$27) \quad \frac{I}{I_o} = e^{-2(X_1 [\alpha + \alpha_{sol} - \alpha_r] + X_2 \alpha_r)}$$

$\frac{I}{I_o}$ expressed in terms of db can be obtained as follows: based on the fact that $db = 20 \log \frac{I}{I_o}$,

$$20 \log \frac{I}{I_o} = db = \frac{-20}{2.303} \times 2 \, (X_1 [\alpha + \alpha_{sol} - \alpha_r] + X_2 \alpha_r)$$

therefore:

$$28) \quad db = -17.369 \, (X_1 [\alpha + \alpha_{sol} - \alpha_r] + X_2 \alpha_r)$$

In practice X_1 is moved and X_2 is kept constant. It is then possible to get an expression in terms of the change in attenuation (db) per change of X_1. Equation 28 then becomes:

$$29) \quad -\frac{\Delta db}{\Delta X_1 (17.37)} = \alpha_{sol} - \alpha_r + \alpha$$

Since the solvent is usually the same as the reference, α_{sol} and α_r cancel, leaving the value of α to be:

$$30) \quad \alpha = \frac{-\Delta db}{\Delta X (17.37)}$$

Data are collected in terms of α at a variety of frequencies and plotted as prescribed by equation 23. One can then obtain τ, the relaxation time, from equation 24.

General Description of the Ultrasonic Instrument

An ultrasonic wave is an acoustic wave with a frequency which is higher than the usual upper limit of the audio frequency (approximately 10 KHz). Although this can mean frequencies up to and including microwave frequencies, in practice the upper limit is considered to be several hundred MHz. A block diagram of this instrument is shown in Figure 3. This includes the components needed to transmit two out-of-phase radio frequency pulses (R. F.) through an acoustical transducing cell and then measuring the attenuation encountered.

In order to induce an acoustic wave of a determined frequency, an acoustic transducer of some sort is required. A way of returning the acoustical wave to some form which can be measured is also required. The method of choice is a pair of x-cut quartz crystals which are mounted on a drop plate that face each other. These crystals are first coated with a layer of chromium, then a layer of gold on both sides. This enables electrical contact to the crystals to be made. A high powered radio frequency signal is applied to the crystal causing it to vibrate at that frequency. This in turn will propagate a pressure wave through the medium to the other quartz crystal where it is again transduced back to a voltage wave.

The quartz crystal becomes a reactive part of an oscillator circuit and will be discussed in further detail. However, it is important to note that the crystals themselves,

FIGURE 3

A block diagram of the ultrasonic instrument.

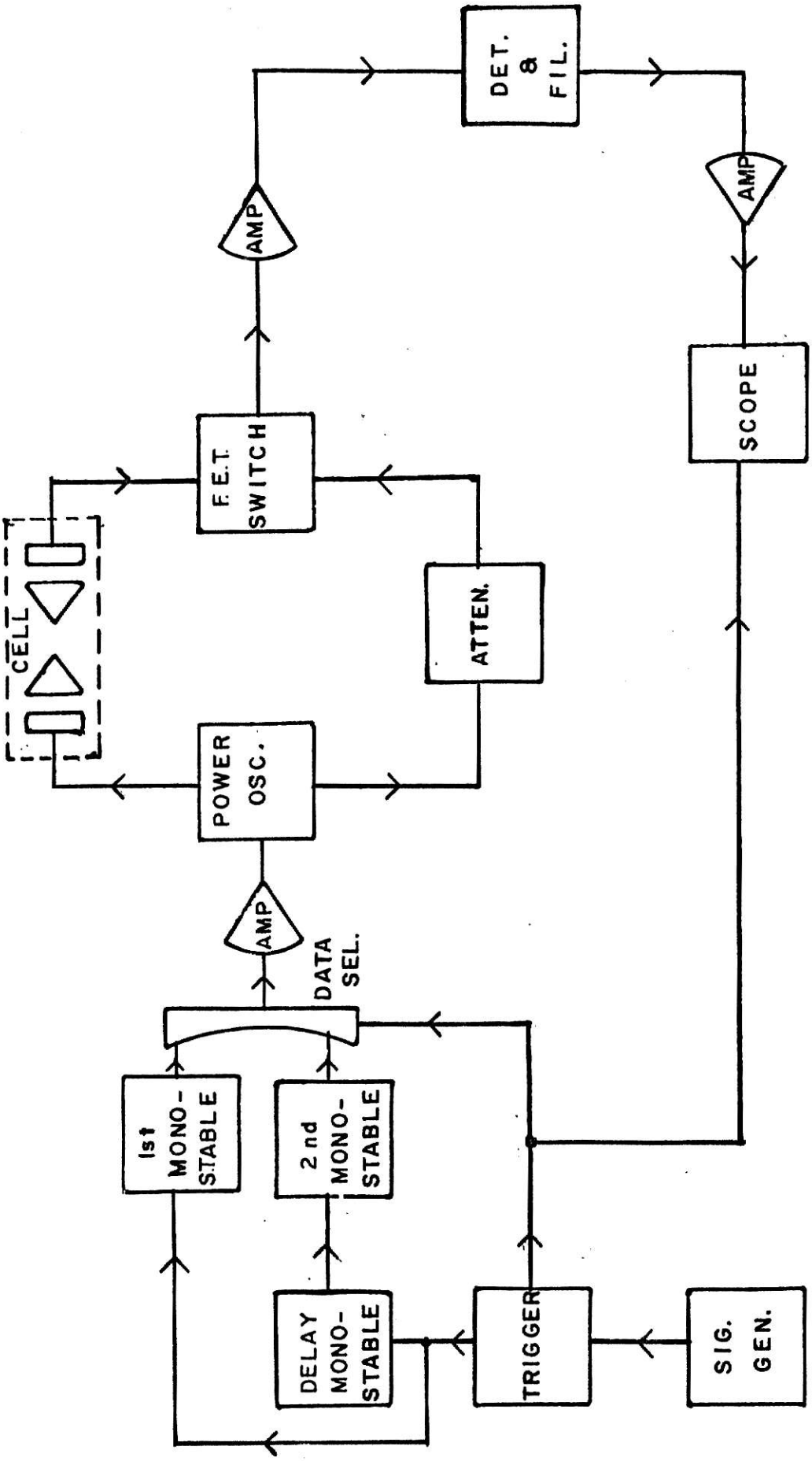
DET. & FIL.
AMP
AMP
SCOPE
F.E.T. SWITCH
CELL
ATTEN.
POWER OSC.
AMP
DATA SEL.
1st MONO-STABLE
2nd MONO-STABLE
DELAY MONO-STABLE
TRIGGER
SIG. GEN.

have a fundamental frequency of vibration. This is determined by the thickness of the crystals and is found by:

$$31) \quad f = \frac{2,870,000}{d} \text{ Hz}$$

where d is the thickness in millimeters (11). In the case of the crystals in this instrument, d is 5.74 millimeters.

The crystals used in this work are 500 KHz, and can be driven to oscillate at higher harmonics. Although the crystals will vibrate at every harmonic, it is only the odd harmonics which will transduce pressure waves to the solution. These are 1.5, 2.5, 3.5...9.5 MHz. This is because of the standing wave configuration at the odd and even harmonics. The nodes of the even harmonics occur at the face of the crystals which corresponds to a zero amplitude while the nodes of the odd harmonics occur at the center of the crystals. This results in maximum amplitude at the face of the crystals for odd harmonics. In theory, one should be able to drive the crystals at all frequencies above the fundamental harmonics but this requires a great deal of power and most crystal configurations are incapable of dissipating the heat generated by the power requirement to do this.

There are two ways in which the signal can be applied to the transducers: either a continuous wave (C. W.) or a pulsed wave. The pulsed system is the one of choice in this application because a continuous wave would be more prone to echoes and reflection (both destructive and non-destructive)

and because it is feared that excess vibrations would cause excessive heat and crack the crystals.

A vacuum tube power oscillator of variable frequency was used. This enables us to pulse the signal at the screen of the tube using a low voltage square wave. (See Figure 11). A tuning capacitor enables us to "fine tune" to what ever harmonic of the 500 KHz crystal we choose. The range of the oscillator is approximately 1 to 20 MHz but can easily be expanded to any frequency range desired.

The pulse generator involves a several step process. This is necessary because two independent pulses are needed. One pulse is a high voltage pulse which drives the crystal transducer and the other is a low voltage pulse which passes through a calibrated attenuator network. The width of each pulse can be varied as can the delay time between the two. The incoming pulses enter the power oscillator at different times through one cable. This is accomplished by data multiplexing. The oscillator itself has a high voltage output and a low voltage output. The two signals pass through the sample and the attenuator, respectively, and are then demultiplexed and the signals fed into a wide band detector. The output is displayed on an oscilloscope as two out-of-phase gaussian curves with the phase shift corresponding to the initial delay time between the two pulses.

Measurements are then made based on the height of the peaks which is a direct measurement of signal strength. In its experimental use, the crystals, which are at a fixed

distance apart, are initially moved so that the transmitting crystal is near the membrane. This means the signal is traveling mostly through the reference solution. The amplitude of the signal coming through the cell is matched to the reference signal by adjusting the attenuator, the pulse width, and the magnitude of the R. F. pulse.

The crystals are then moved horizontally with respect to the membrane to some point where the signal passes through more sample and less reference solution. If an absorption has taken place, this would be indicated by a decrease in output amplitude. The attenuator network can now be adjusted to compensate for the attenuation by the sample. The amount of this compensation by the attenuator (in db) divided by the distance the crystal moved is the absorption coefficient in units of $\frac{db}{cm}$.

A detailed description of the instrumentation

In this section schematic diagrams are used to illustrate instrument design. The resistor values are given in ohms and the capacitor values are given in microfarads unless otherwise indicated.

Double pulse generator:

A block diagram of the double pulse generator is shown in Figure 4. The signal generator does not need to have any particular wave form since it goes through a Schmitt trigger but it must remain constant. In the past a Wien bridge oscillator was used, however, this particular

FIGURE 4

The block diagram of the double pulse generator.

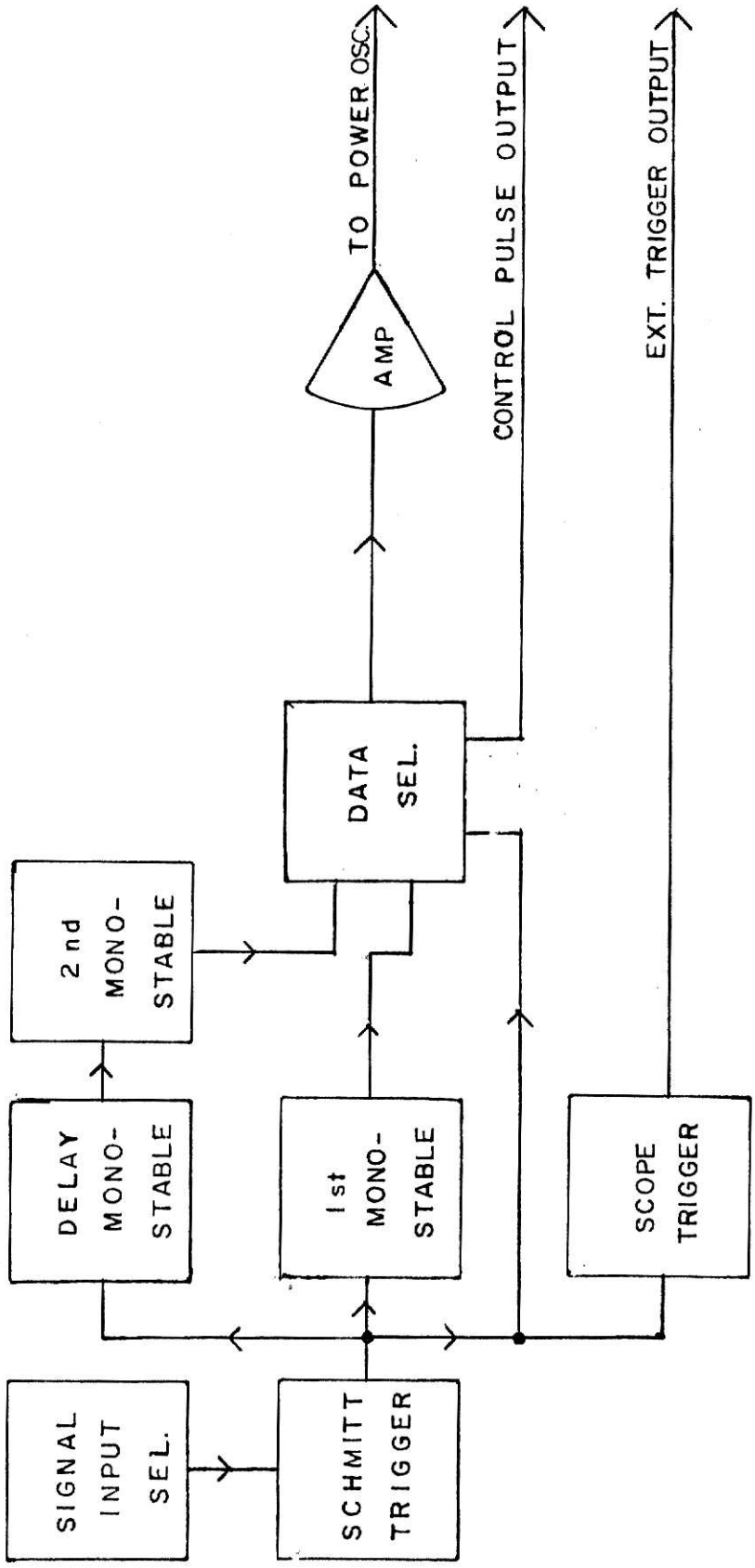
SIGNAL INPUT SEL.
SCHMITT TRIGGER
DELAY MONO-STABLE
2nd MONO-STABLE
1st MONO-STABLE
SCOPE TRIGGER
DATA SEL.
AMP
TO POWER OSC.
CONTROL PULSE OUTPUT
EXT. TRIGGER OUTPUT

configuration was unreliable and failure occurred often. This was replaced by a 555 monolithic timer (12). This is a multipurpose integrated circuit which in this instance is wired in an astable free running oscillator configuration, as shown in Figure 5. The frequency is determined by the resistor-capacitor combination. The frequency is found by:

$$32) \quad f = \frac{1.44}{(R_A + 2R_B)\ C}$$

with

$$R_A = 820 \text{ ohm and } R_B = 5.6K \text{ ohm and } C = 0.1uf$$

The frequency is found to be 1.198 KHz.

A four position rotary switch is used to select either the output of this timer or three other possible frequencies to enter the Schmitt trigger:

1) 120 Hz

2) 60 Hz

from a full and half wave rectified AC voltage from a filament transformer, or

3) An external source input.

This configuration is shown in Figure 6.

The Schmitt trigger is a basic type shown in Figure 7. The output of this Schmitt trigger is a 5 volt square wave. This triggers four other devices:

FIGURE 5

The schematic of the 555 oscillator.

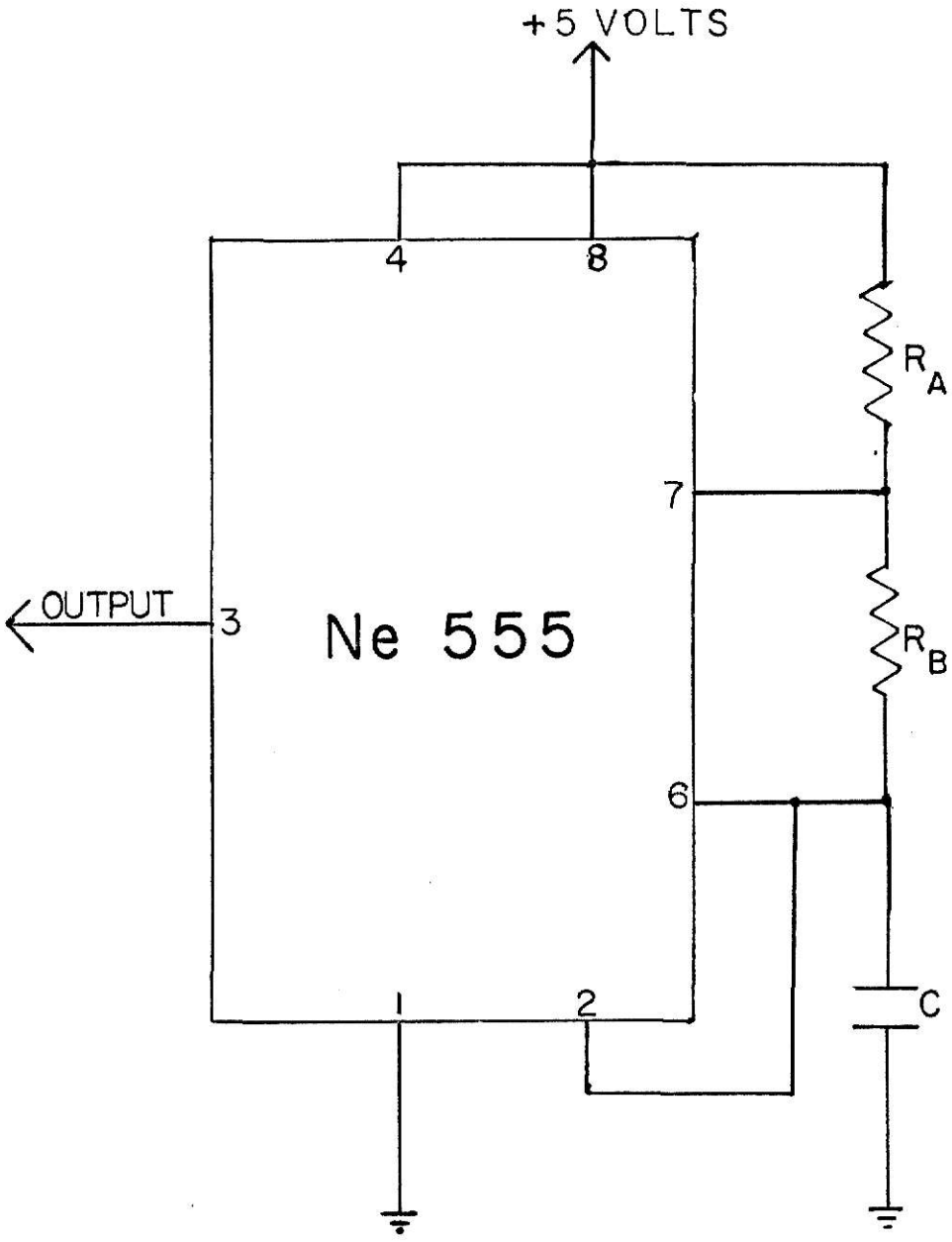
+5 VOLTS
4
8
R_A
7
OUTPUT
3
Ne 555
R_B
6
1
2
C

THIS BOOK CONTAINS NUMEROUS PAGES THAT ARE CUT OFF

THIS IS AS RECEIVED FROM THE CUSTOMER

FIGURE 6

Schematic of the signal selection network.

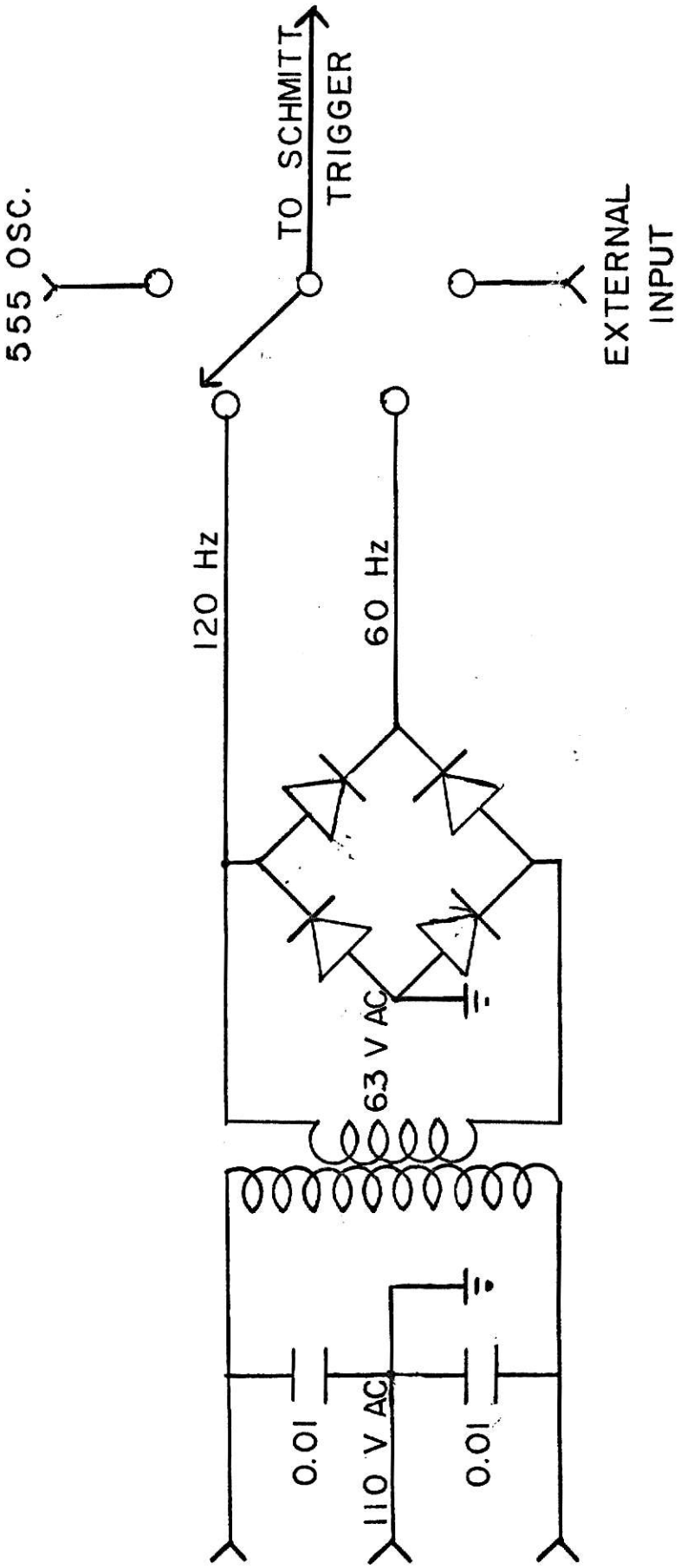
555 OSC.
TO SCHMITT TRIGGER
EXTERNAL INPUT
120 Hz
60 Hz
63 V AC
0.01
110 V AC
0.01

FIGURE 7

Schematic of the Schmitt trigger.

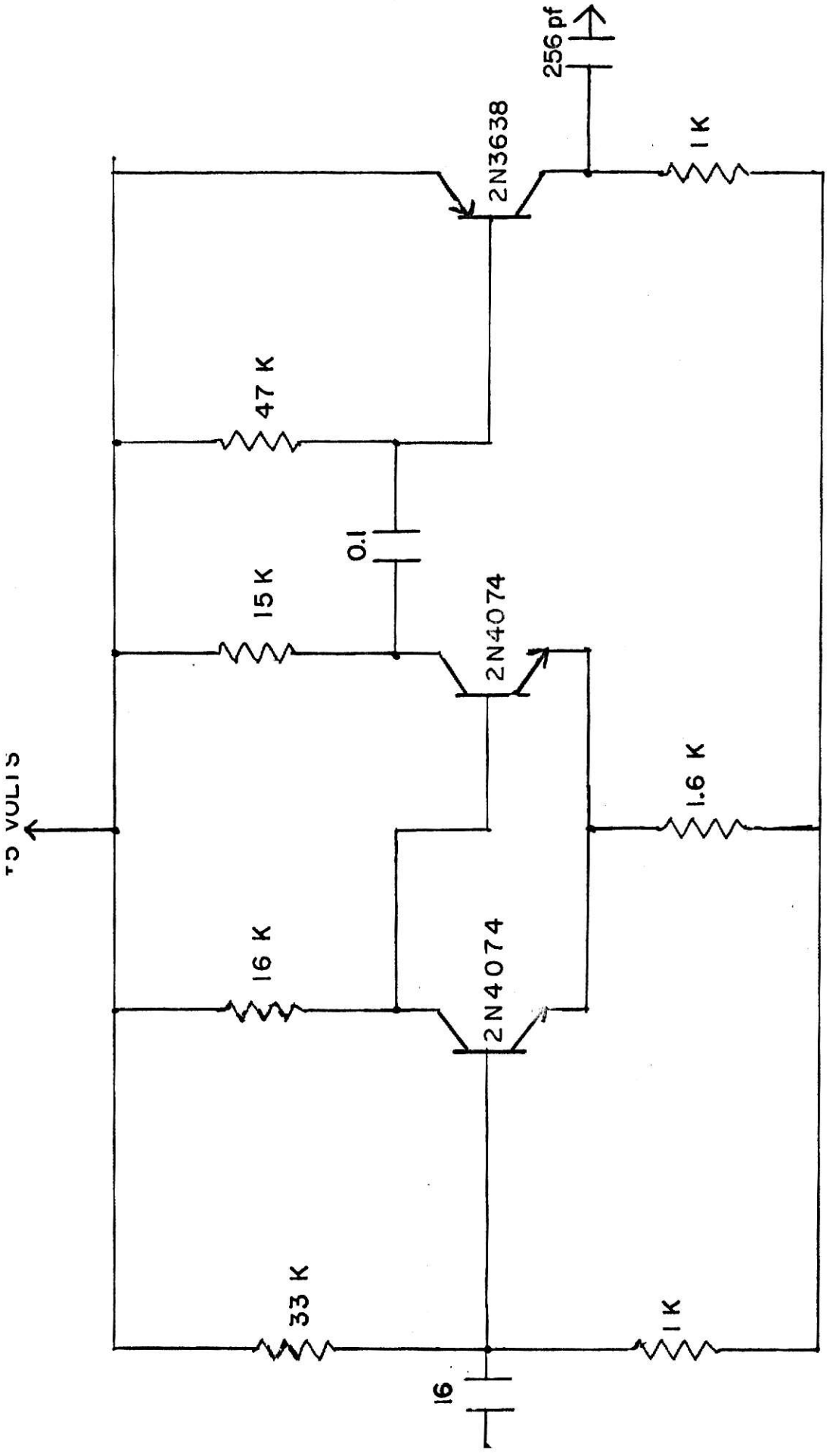
256 pf
2N3638
1 K
47 K
0.1
15 K
2N4074
TO VULIS
1.6 K
16 K
2N4074
33 K
1 K
16

1) Oscilloscope trigger (Figure 8)

2) Monostable multi-vibrator (Figure 9)

3) Delay monostable multi-vibrator (Figure 9)

4) Clock signal to data select logic (Figure 10)

There are three discrete monostable multi-vibrators, two of which are identical and the third which differs by non-inversion of the output.

The Schmitt trigger will trip both the first monostable multi-vibrator and delay monostable multi-vibrator simultaneously. The delay monostable multi-vibrator will in turn trip the second monostable multi-vibrator. A schematic of the first and the second monostable multi-vibrator is shown in Figure 9. The delay monostable multi-vibrator is identical except the output is taken at point A rather than point B. These are edge trigger devices; that is, a rising edge trips the pulse which will remain on for a determined length of time. This time is controlled by a 1K ohm potentiometer which adjusts the amount of feed back voltage. This effects the charging of a capacitor. The first monostable multi-vibrator and the second monostable multi-vibrator produce positive pulses with an incoming rising edge and the delay monostable multi-vibrator gives a negative pulse with an incoming rising edge. This means that if the first pulse and the delay pulse trip simultaneously, one will be the inverse of the other. The positive going edge of the delay pulse will trip the second monostable multi-vibrator. Hence, the pulse width of the delay monostable

FIGURE 8

Schematic of the oscilloscope trigger.

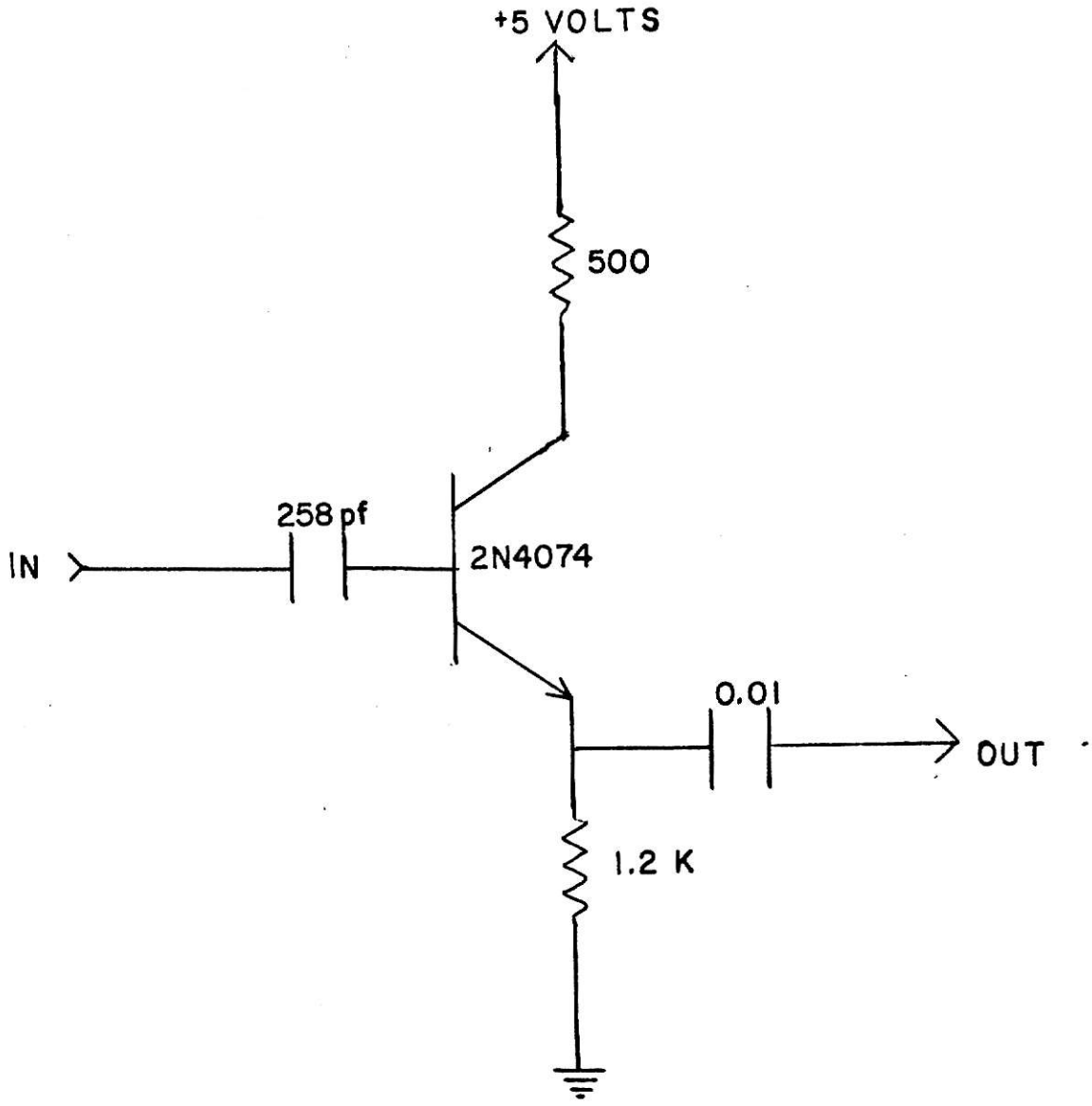
+5 VOLTS
500
258 pf
IN
2N4074
0.01
OUT
1.2 K

FIGURE 9

The schematic of the monostable multi-vibrator with the delay output at A and the first and the second output at B.

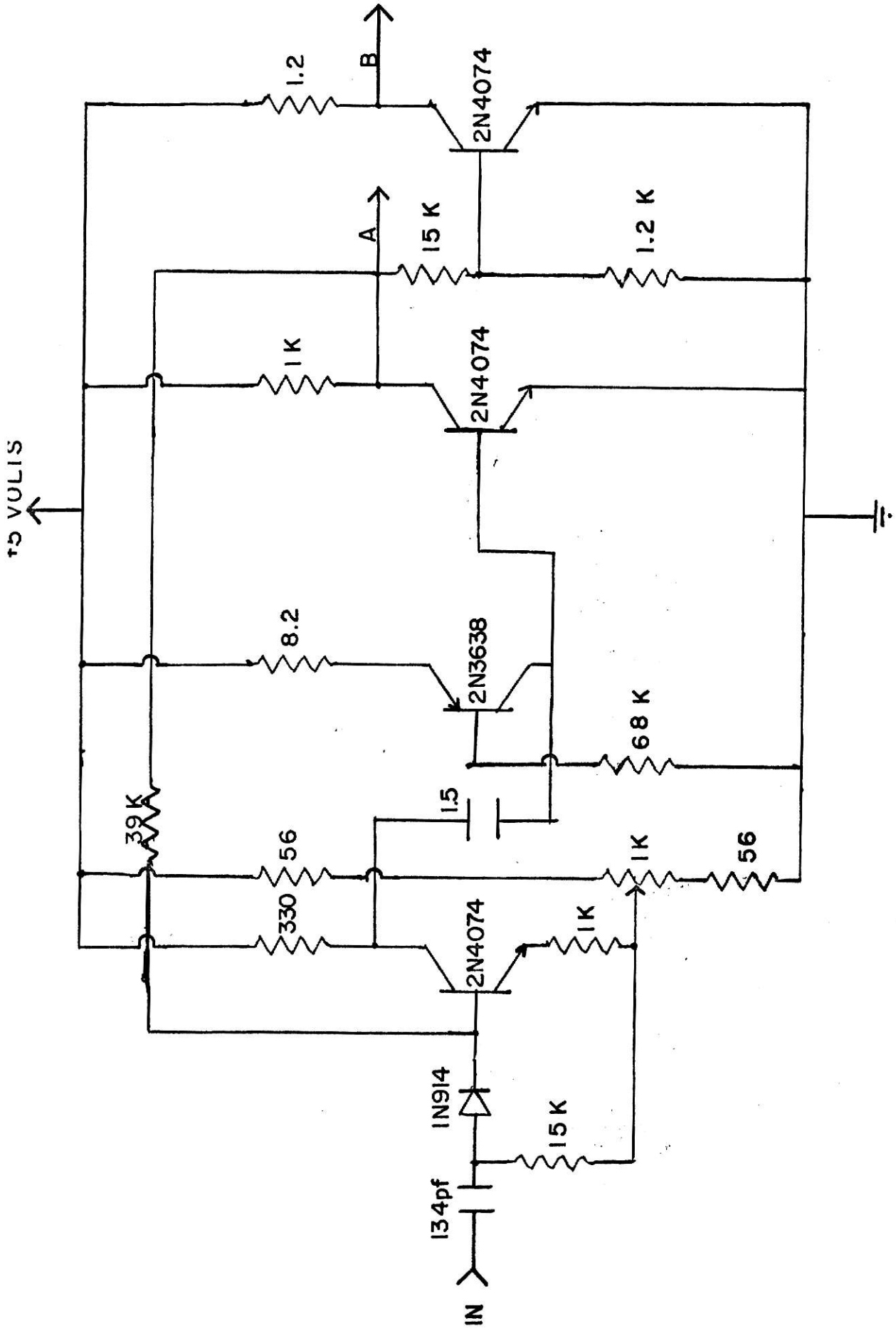
TO VULIS
1.2
B
2N4074
A
15 K
1.2 K
1 K
2N4074
8.2
2N3638
68 K
39 K
1.5
56
1 K
56
330
2N4074
1 K
1N914
15 K
134pf
IN

FIGURE 10

A schematic of the data select network.

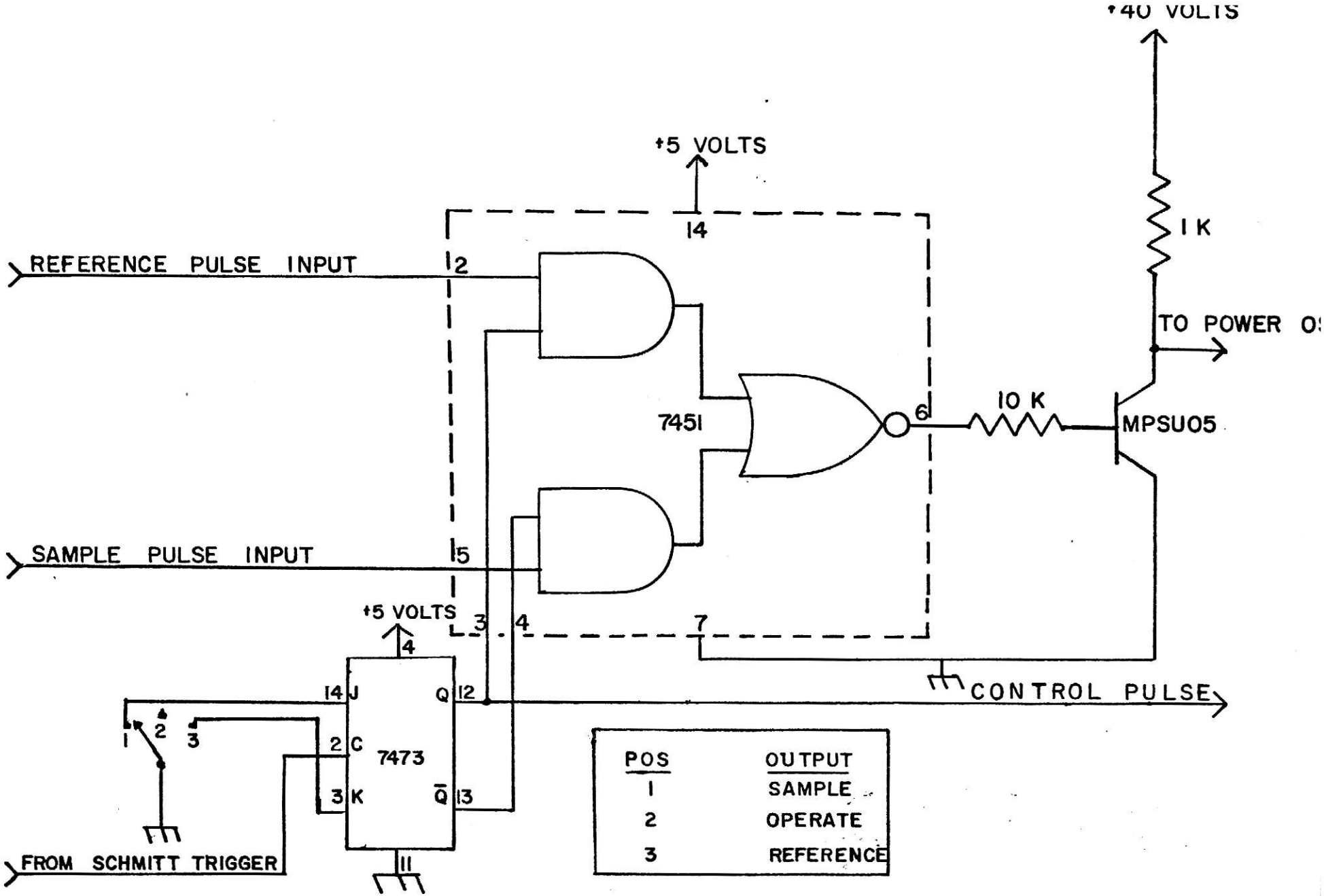
+40 VOLTS
+5 VOLTS
14
1 K
REFERENCE PULSE INPUT
2
TO POWER O
7451
6
10 K
MPSU05
SAMPLE PULSE INPUT
5
+5 VOLTS
3
4
7
4
CONTROL PULSE
14 J
Q 12
1
2
3
2 C
7473
3 K
Q 13
FROM SCHMITT TRIGGER
11
POS
OUTPUT
1
SAMPLE
2
OPERATE
3
REFERENCE

multi-vibrator, in fact, determines the delay time. The width of both the first and the second pulses are adjustable with their own 1K ohm potentiometer. The pulse width of the first and the second monostable multi-vibrator are adjustable from 0 to 120 micro-seconds and the delay between them can be 0 to 140 micro-seconds. In actual use these values will vary because the delay which is encountered by the signal passing through the sample will not remain constant and will vary from sample to sample.

It will be shown shortly, that both the first and the second pulses need to be fed into one input of the power oscillator. This is done by data multiplexing. Since there are only two bits of information, the 7451 "and-or-invert" gate (12) was used with a J. K. Flip-Flop to provide the selection information. The clock rate of the Flip-Flop will determine at what rate the data are sampled. The Schmitt trigger is well suited for the clock because the rate is such that the eye will not detect the switching and thus will appear to be simultaneous when you observe the results on the oscilloscope. A schematic of the data select network is shown in Figure 10. Note that the Q output of the Flip-Flop also goes out to the control pulse of the receiving unit. This is necessary to assure that the receiver "looks" at the right signal at the right time. The output of this network goes into a single stage pulse amplifier which inverts the pulses and amplifies them to +40 volts which provides adequate power to pulse the power oscillator.

Power Oscillator

The power oscillator is a combination of several types of configurations and closely resembles the Colpit oscillator. The schematic is shown in Figure 11. This is a much simplified version of that which was originally used by Ford. Note that the screen is pulsed rather than the grid, as is commonly done. This eliminates the need for a negative bias supply which distorted the pulses. The output has been modified to provide both a high voltage R. F. pulse and a low voltage pulse. The variable capacitor at the output is used to adjust the final signals to be the same. Each output will show both the first and second pulse but the receiver has the appropriate demultiplexing logic so the high voltage first pulse is looked at through the sample, while the low voltage second pulse is looked at through the attenuator network. This perhaps has been the most significant improvement because this eliminates the need for calibrated reference oscillators. The reference signal is taken right off the power oscillator, which means any deviations in one will coincide precisely with the other, thus negating the effect. It should be noted at this point that the high voltage pulse is in the order of 300 volts peak to peak, while the low voltage pulse is in the order of 30 millivolts but by the time the high voltage pulse passes through the cell, it is attenuated to the point where it is now 20 - 50 millivolts. Hence, the high voltage and the low voltage pulse are of the same order of magnitude by the time

FIGURE 11

The schematic of the power oscillator.

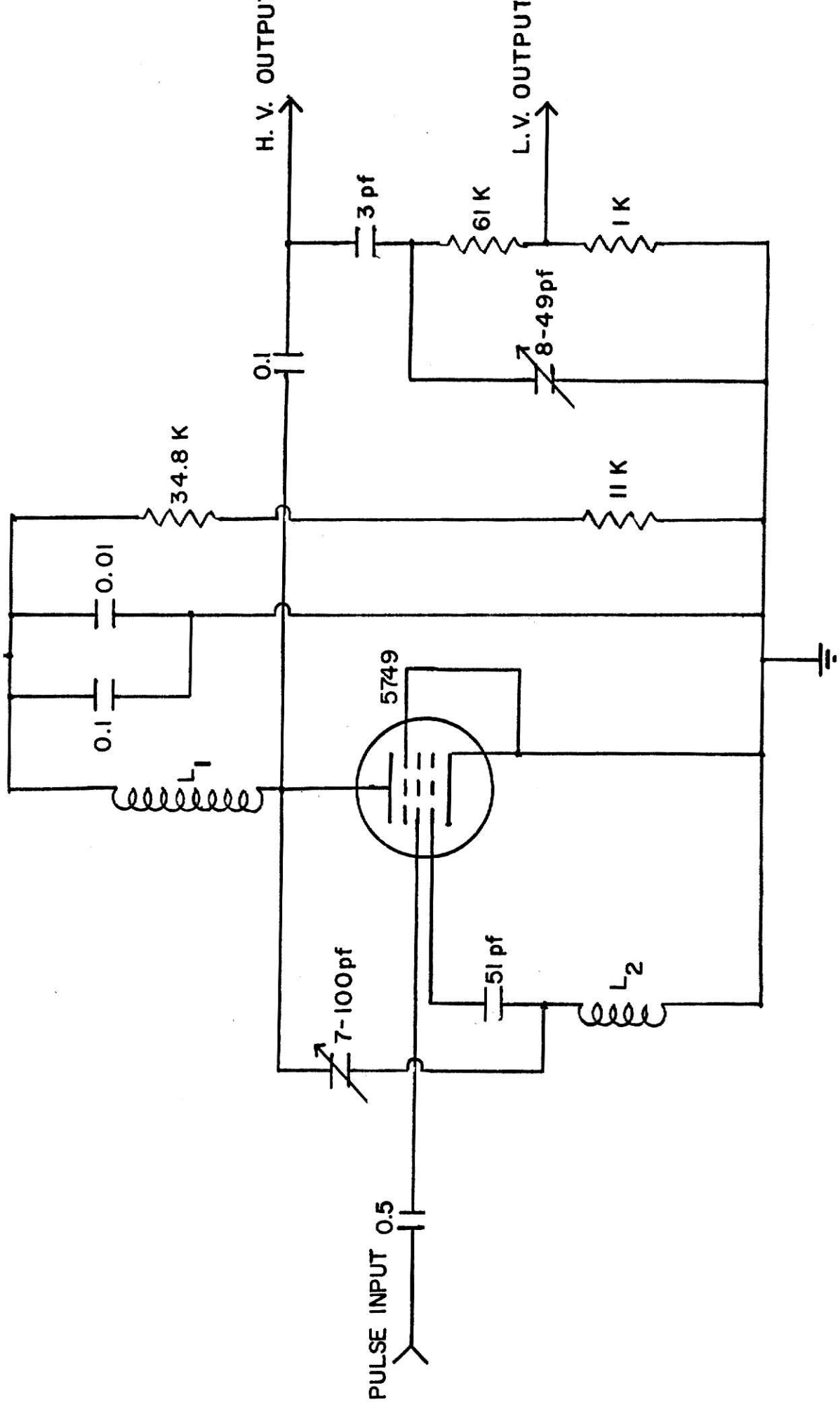
H. V. OUTPUT
L.V. OUTPUT
3 pf
61 K
1 K
8-49pf
0.1
34.8 K
11 K
0.01
0.1
5749
L_1
L_2
51 pf
7-100pf
0.5
PULSE INPUT

they reach the receiver.

The attenuator network:

The attenuator network is a commercially available device made by the Daven Company of Newark, New Jersey. It has an input impedance of 75 ohms and a frequency range of 0 to 225 MHz and can attenuate signals up to 100 db in increments of 0.1 db.

The receiver:

The receiver has an input switching network at the front end for demultiplexing purposes. Field effect transistors (FETS) are used for this rather than digital logic as in the transmitter because now analog (R. F.) signals are being switched and must retain all of their AC, dipolar characteristics. Figure 12 shows the schematic of this network. The incoming control pulse which originated at the Q output of the Flip-Flop shown in Figure 10, sets up an RCA CA3046 transistor array package (13), which in turn provides proper gating information to 4 n-channel FETS (2N4416). These 4 FETS provide an electronic double pole double throw switch. This circuit provides a low impedance path to ground for the signal not selected while allowing the selected signal to pass through to the receiver without distortion.

The receiver itself is compiled of four sections. This schematic is shown in Figure 13.

The first section is a wide band R. F. amplifier. The RCA CA 3040 wide band amplifier integrated circuit package

FIGURE 12

The schematic of the FET R. F. switching network.

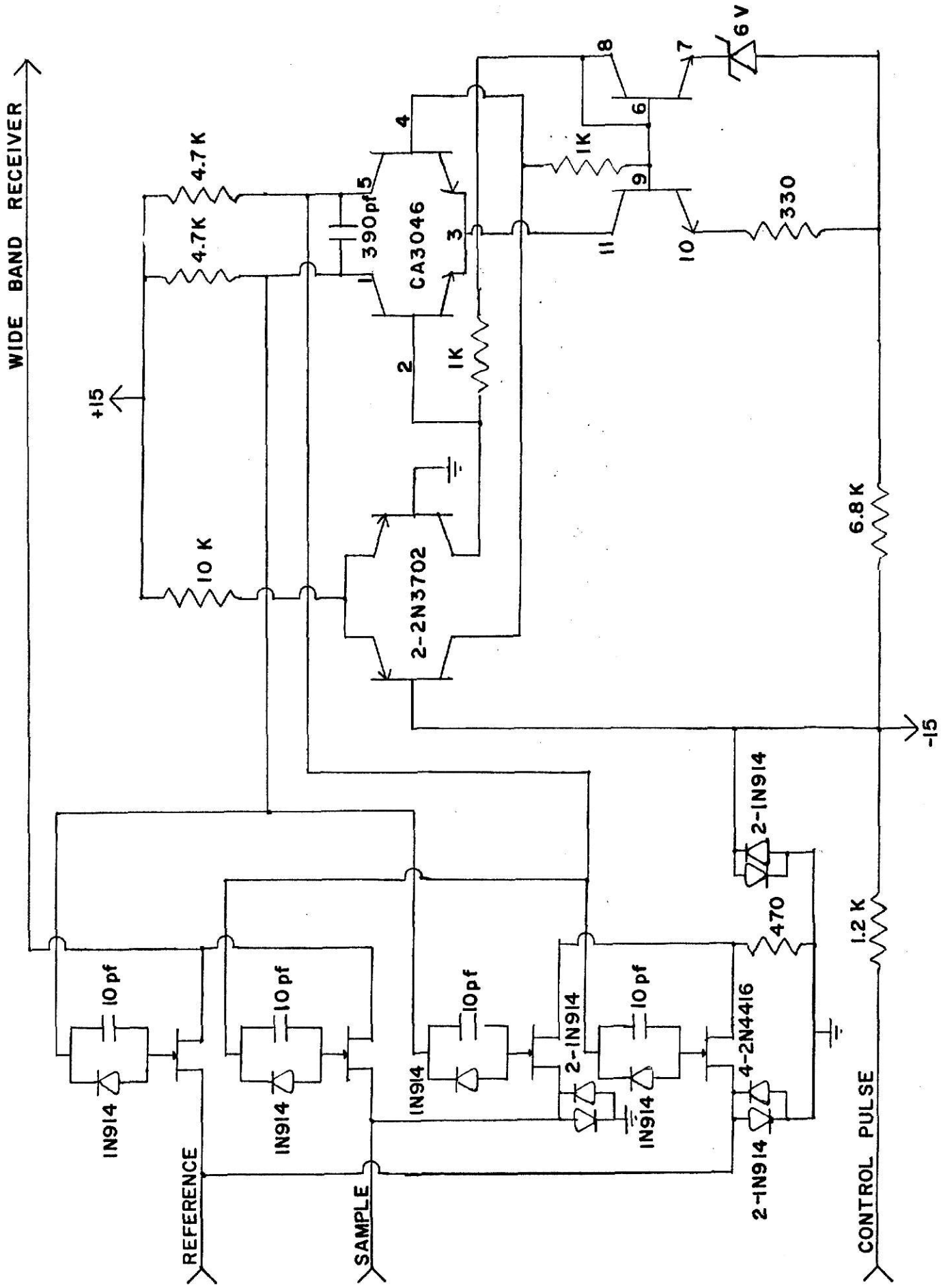
WIDE BAND RECEIVER
+15
-15
4.7 K
4.7K
10 K
390pf
CA3046
1K
2-2N3702
1K
330
6 V
6.8 K
1.2 K
470
10 pf
IN914
2-IN914
4-2N4416
REFERENCE
SAMPLE
CONTROL PULSE

FIGURE 13

The schematic of the wide band receiver.

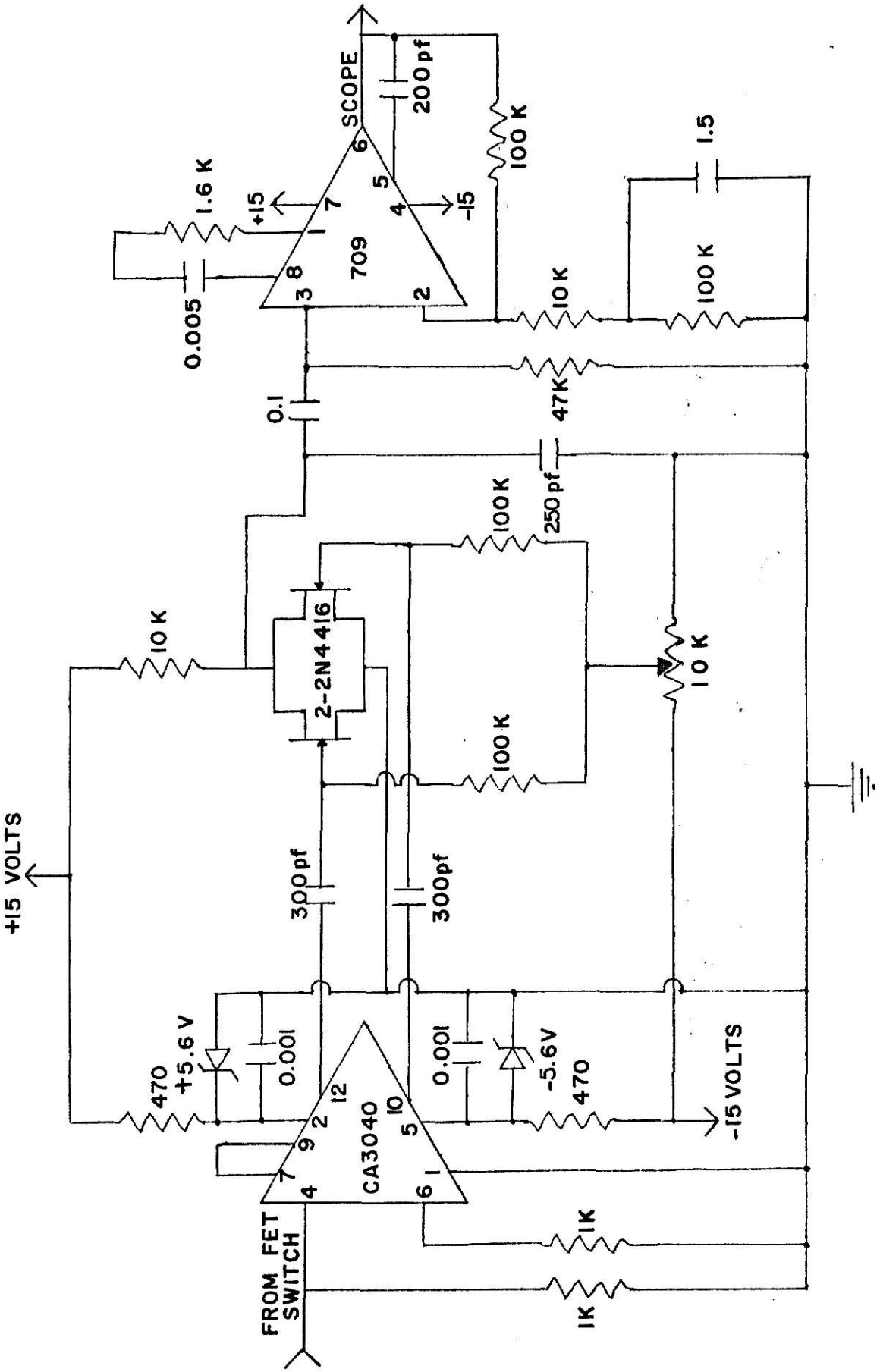
SCOPE
200 pf
100 K
1.5
1.6 K
+15
-15
709
0.005
10 K
100 K
0.1
47K
250 pf
100 K
10 K
2-2N4416
10 K
100 K
+15 VOLTS
300 pf
300pf
470
+5.6 V
0.001
0.001
-5.6V
470
-15 VOLTS
CA3040
FROM FET SWITCH
1K
1K

is used here (13). This is capable of amplifing signals up to 200 MHz. The design used here eliminates the need for tuned video amplifiers at the higher frequencies, as was needed in the past. This device operates on ± 6 volt supply, while the rest of the circuitry operates on ± 15 volts. To satisfy this situation a 5.6 volt zener diode voltage supply was used, thus enabling the entire receiver unit to operate from a single ± 15 volt modular supply.

The second section of the receiver is the video detector. The purpose of this is to detect the amplified R. F. signals and convert them to a DC signal which is proportional to the intensity of the input. The result of this is a wave form which resembles the positive portion of the envelope containing the R. F. pulse. The detection device used previously in this application was a diode rectifier which literally rectifies the incoming signal to DC. This has the disadvantage of being unable to see any signal below its threshold voltage (1 diode drop). It also does not have the speed which would be required for high frequencies. The type of detector now used is a dual n-channel FET square law detector. The principle of this detector is based on the square law properties inherent in all FETS. The drain current of the FETS are directly proportional to the incoming signal. This current is measured by a three term expression:

$$33) \quad V_{in} \propto I_d = V_{ac} + V_{dc} + A^2 \sin^2 \omega t$$

V_{in} is the incoming R. F. signal and I_d is the drain current. V_{ac} is an AC term which will cancel due to the symmetry of the detector. V_{dc} is a DC term upon which $A^2 \sin^2 \omega t$ is superimposed. An equivelant expression would then be:

$$34) \quad I_d = V_{dc} + \tfrac{1}{2}A^2 - \tfrac{1}{2}A^2 \cos 2\omega t$$

The cosine term is removed by a low pass filter, with a time constant of 2 micro seconds. This removes all AC above 500 KHz. The FETS are biased by two 10K ohm trimmer potentiometers. The final section of the receiver is a video amplifier which amplifies the filtered signal to approximately 6 to 8 volt peaks, which at this point appear Gaussion. A Fairchild 709 operational amplifier was used in a "follower with gain" configuration (14). The entire receiving unit, including the switch network, was laid out on a single printed circuit board, the lay out of which is shown in Figure 14.

Data Recording

The primary device used for measuring peak heights is a Tektronic, Inc. type 531A oscilloscope. This has a type 1A2 dual trace plug-in module. This is a 15 MHz scope with a rise time of 0.022 microseconds. The scope is set to trigger externally from the trigger pulse shown in Figure 8.

Detailed description of the cell

The cell which was previously shown in Figure 2 is basically the type used by Corsaro, Atkinson, and Perlis (10). The sample container is equipped with a water jacket so isothermal

FIGURE 14

The printed circuit board layout for the receivers.

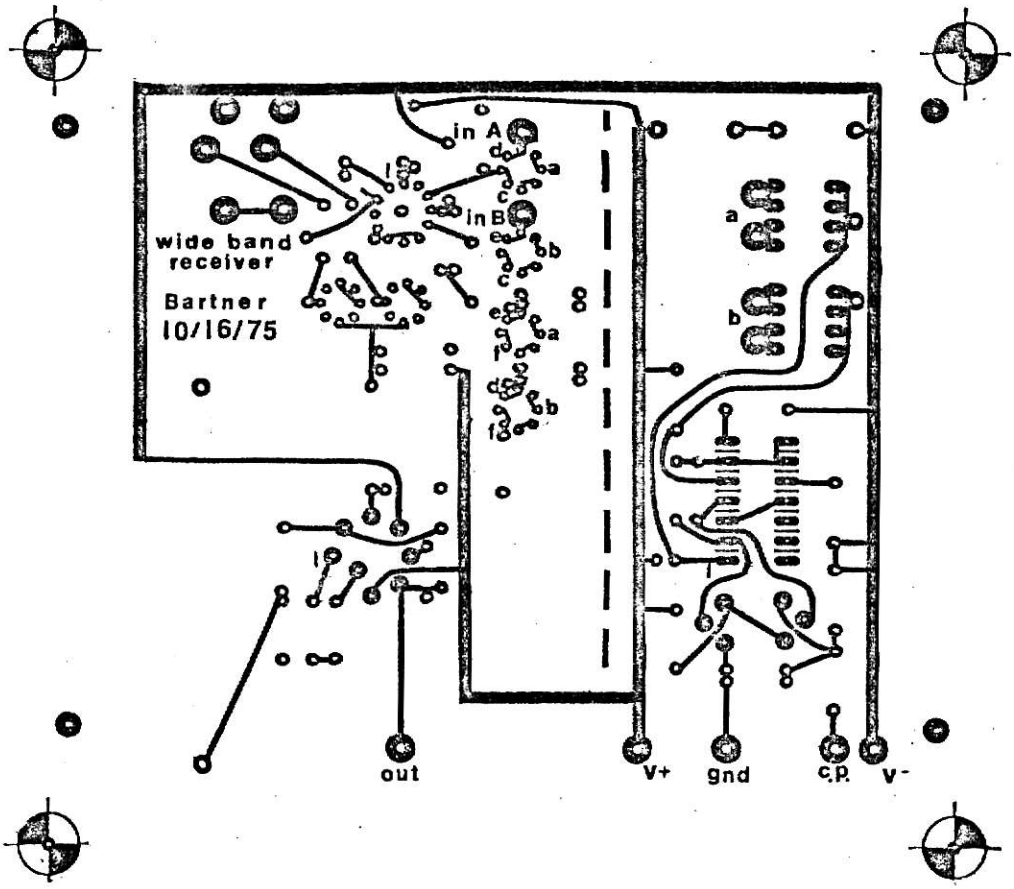
wide band
receiver
Bartner
10/16/75
in A
in B
out
V+
gnd
c.p.
V-

conditions may be maintained. Water from a Sargent-Welch constant temperature bath is circulated through the cell by an immersion pump. The bath can regulate temperature to within a 0.01°C. There are two halves of the cell which are divided by a semi-permeable membrane which is permeated only by the ultrasonic waves. Each compartment will hold approximately 500 milliliters of solution. In practice, the right side is filled with the solvent of the system and the left side contains the species under study dissolved in the solvent. A view of the cell is shown in Figure 15.

The quartz crystal transducers are mounted in stainless steel crystal holders which were milled especially for this purpose and are spring loaded and adjustable to maintain the two crystal faces parallel. This is shown in Figure 16A and 16B. The crystal transducers are mounted on a steel drop plate in such a way that the crystals face each other and are parallel. A view of this is shown in Figure 16C. The drop plate is mounted on a block of aluminum which is driven by a ¼ inch diameter threaded steel rod. This drive screw has 13 threads per inch and is coupled to a motor through a gear arrangement which yields a 3:1 reduction of motor speed. The motor is a General Electric model number 5SMY54HB1. A cog wheel at the left end of the drive screw, trips a micro switch six times per revolution. This in turn is detected by a Sodero type TCeZ5E.97 space 40 ohm pulse counter. This drive system enables the operator to move the crystals horizontally with

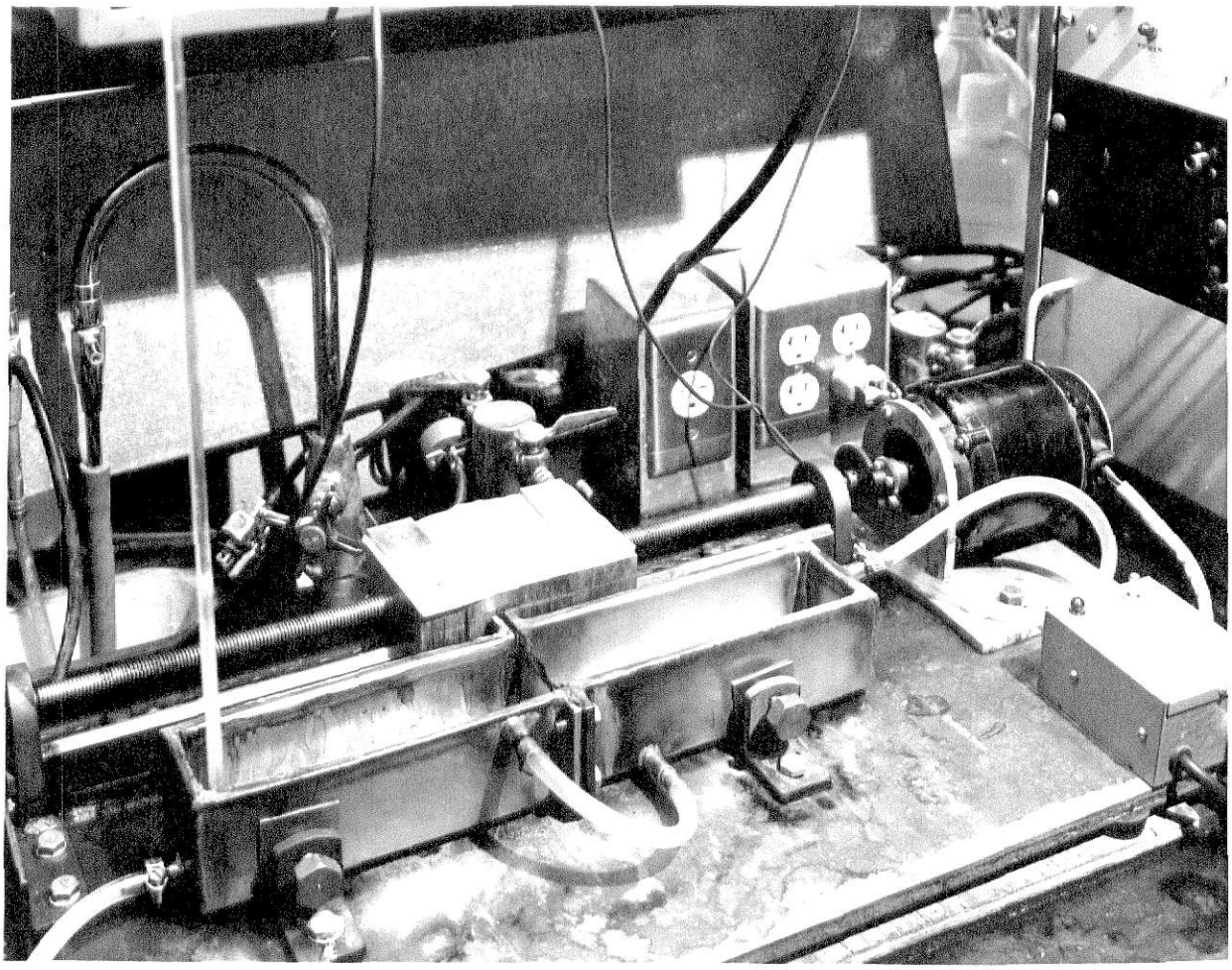

FIGURE 16

A. A view of the crystal transducer in its mounting.

B. A composite view of the crystal and its mounting.

C. A view of the crystal transducers mounted on the drop plate.

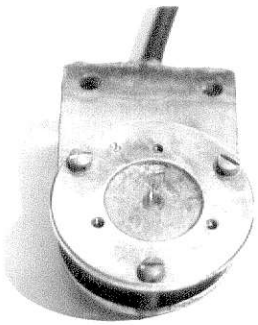

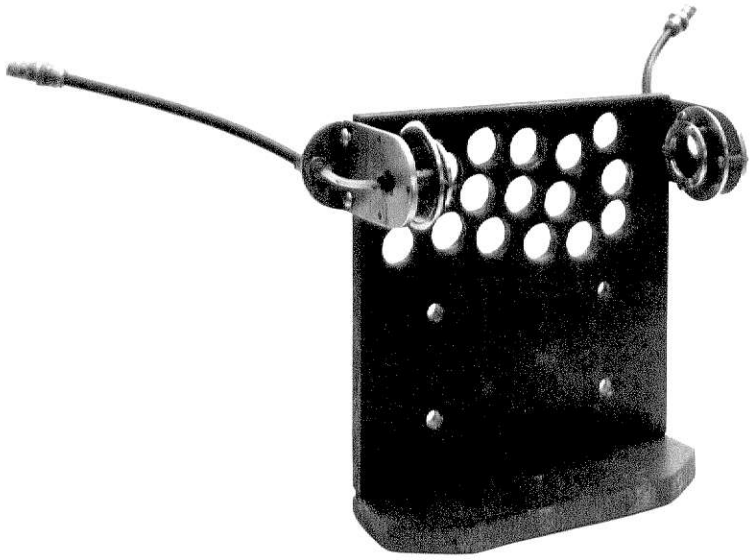

respect to the cell membrane. The conversion factor for translating counts to distance in centimeters is given by equation 35.

35) 1 count = 0.03258 cm

The quartz crystals are a reactive part of the oscillator circuit and therefore the equivalent circuit must be considered. This is shown in Figure 17. The values of the components shown depend mostly on the resonance properties of the quartz, but the mounting and loading of the crystals also are important. C_1 is a function of the type of mounting. Because of the type used here, this value is larger than the author anticipated; 27 picofarads. This total value includes the capacitor values of the crystal, the mounting, and the coaxial lead-in cable (RG 59U cable). R, C_2, and L are a function of the quartz. R has a value of 12 ohms, C_2 has a value of a few picofarads, and L is in the order of several Henries. These values can be measured on a bridge circuit in solution and will vary from solution to solution.

The crystal mounts were milled to have a minimum contact area with the crystal to give low damping. The mount is at electrical ground, thus the front face of the crystal is at ground. A Teflon spacer is used to insulate the rear face of the crystal from the mounting. There is a cavity behind the crystal which is partically filled with General Electric silicon cement to give a rough surface and prevent water from entering the coaxial cable. The cable enters through the back

FIGURE 17

The schematic of the equivalent circuit of the quartz crystal.

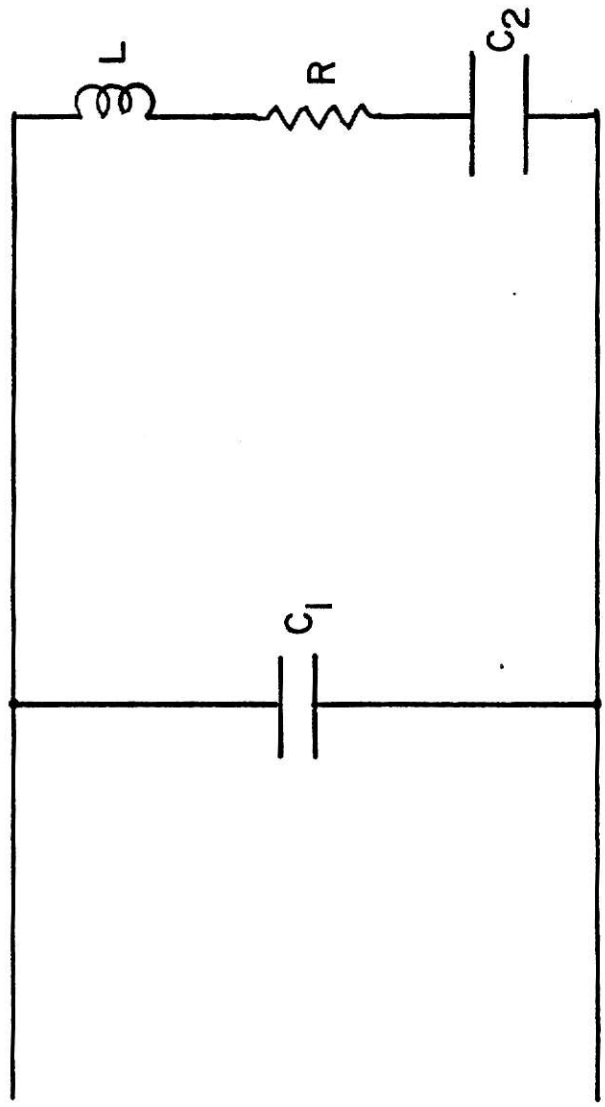
L
R
C2
C1

hole of the mount and is stripped to expose the center lead. The shield is connected to the mount and the center lead is bent to form a modified spring contact. When the crystal is placed over the cavity, the wire will release and make electrical contact with the gold plating on the rear face of the crystal.

The crystals were made by Valpey in Holiston, Mass. They are ground to 500 KHz with a layer of chrome and a layer of gold on each face. They were cut from the x-plane.

Figure 18 shows the view of the completed ultrasonic instrument. Figure 19 shows the profile of the data multiplexing system.

Experimental Procedure

It was hoped that this instrument could be used to determine equilibrium rate constants and activation energies of metal chelate adducts.

Chemical description:

The vanadium benzohydroxamic acid chelate was chosen as the species of study because of its interest to this research group. It has been shown that this chelate forms a ligand to metal ratio of 2:1 as illustrated in Figure 20 (15-16). When dissolved in n-Butanol both solvent and available water adducts will bond to the chelate. It is the energy of these bonds which are to be studied. The preparation of the chelate is as follows: Sodium vanadate (Fisher lot 763885) was dried in a vacuum drying oven for two days at 110°C. Benzohydroxamic acid (Eastman-Kodak lot 771-2A) was dried in a vacuum oven for two days at 50°C. 2 to 1 molar quantities of benzohydroxamic acid and sodium vanadate

FIGURE 18

A view of the ultrasonic instrument.

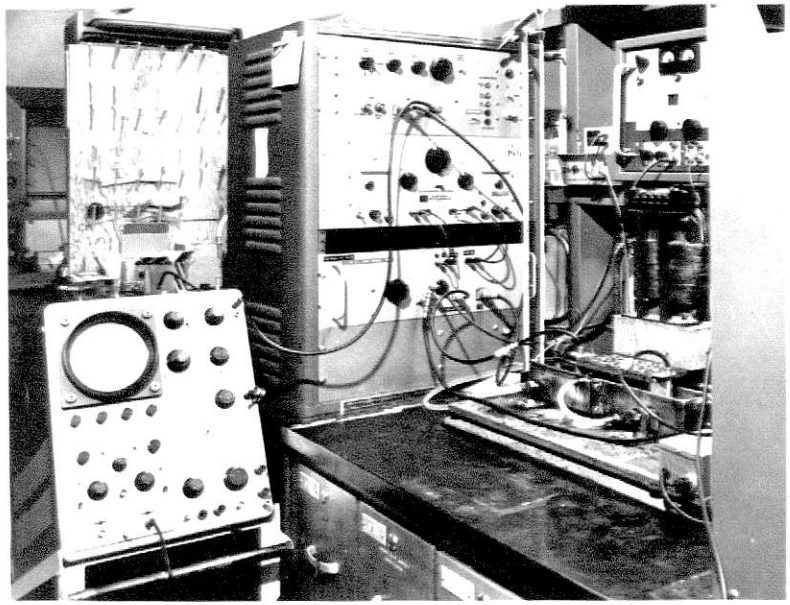

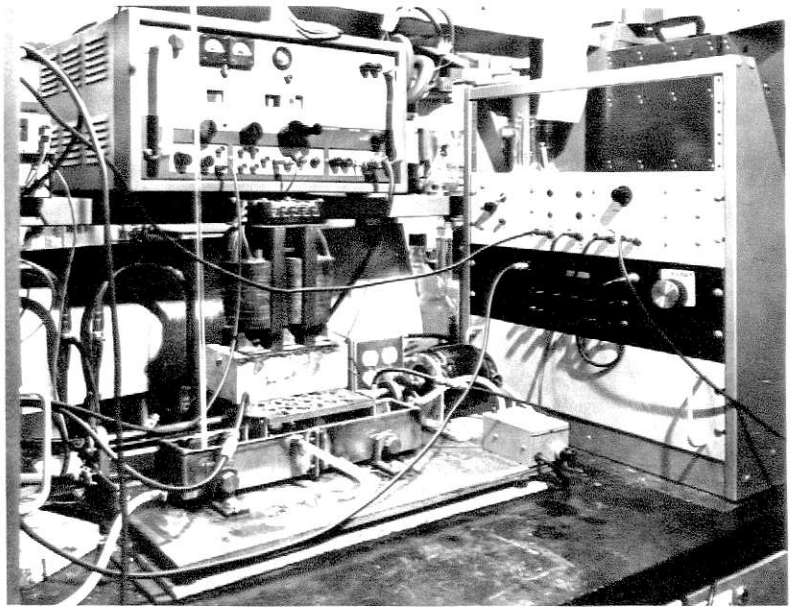

FIGURE 19

The profile of the data selector logic.

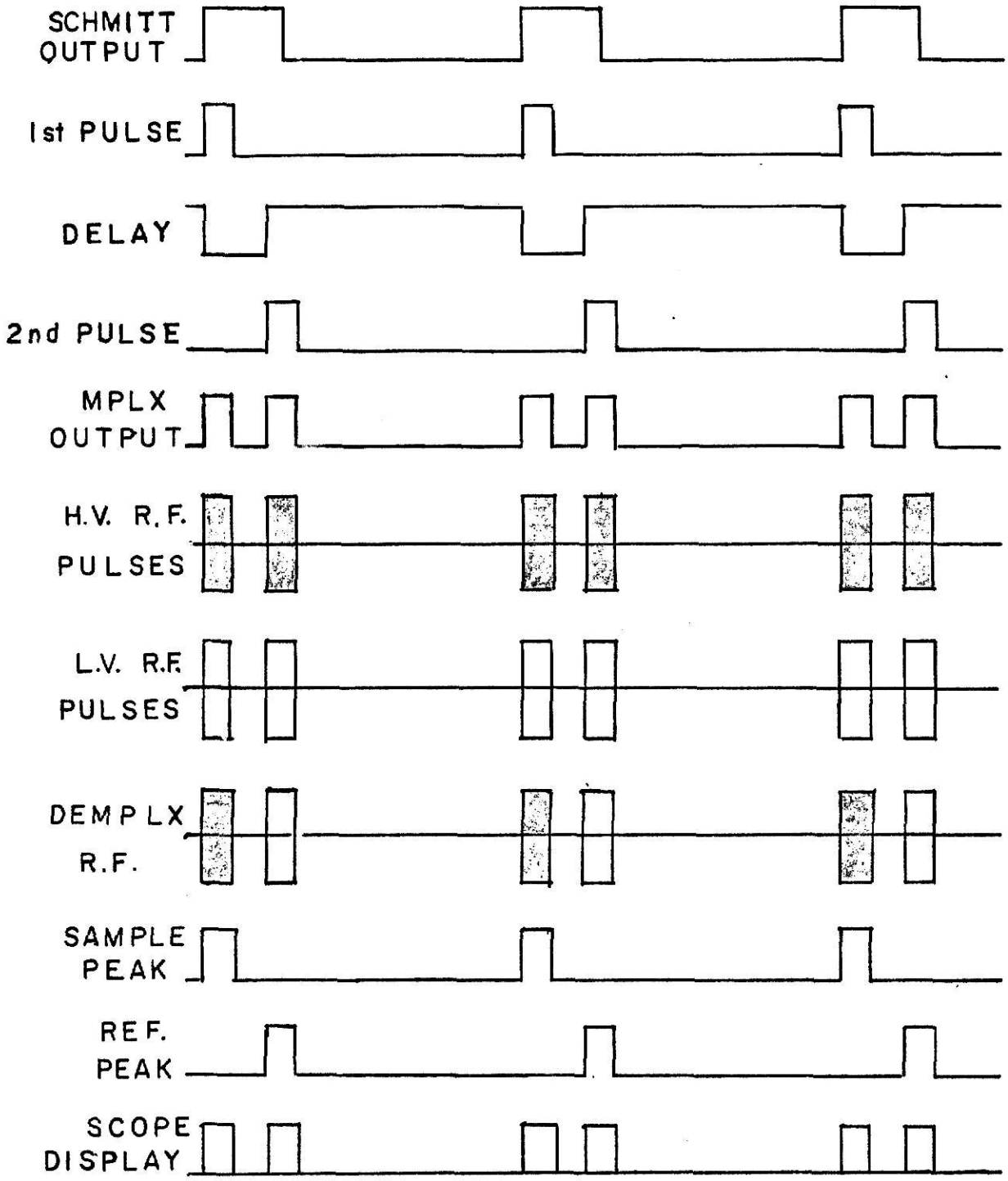
SCHMITT OUTPUT
1st PULSE
DELAY
2nd PULSE
MPLX OUTPUT
H.V. R.F. PULSES
L.V. R.F. PULSES
DEMPLX R.F.
SAMPLE PEAK
REF. PEAK
SCOPE DISPLAY

FIGURE 20

The structure of vanadium benzohydroxamic acid chelate.

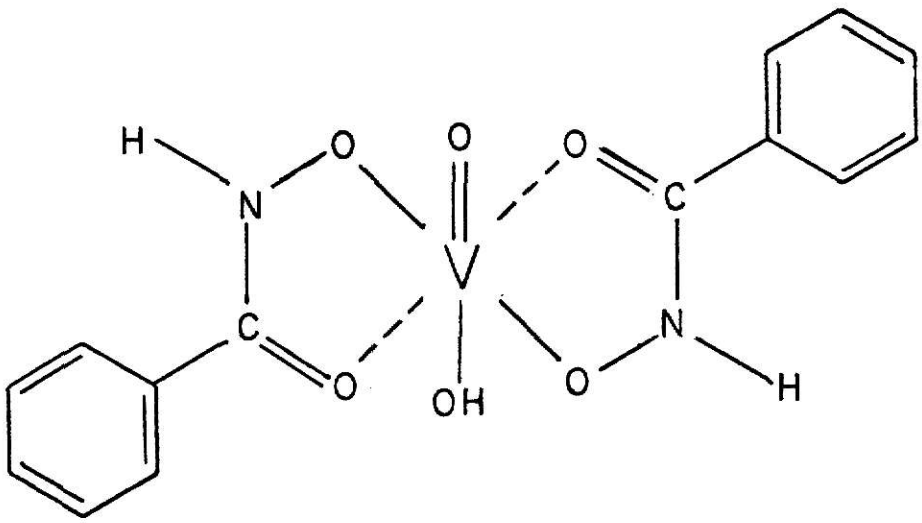
H
O
O
O
C
N
V
C
O
O
OH
O
N
H

respectively were weighed out and each dissolved in 500 ml of distilled-deionized water.

The pH of the sodium vanadate solution was adjusted to 5 with 6M HCl. The benzohydroxamic acid solution was slowly added to the sodium vanadate and the solution gradually changed to a deep purple color as the chelate was formed. The pH of the mixture was further lowered to 2.4 and the resulting precipitate was filtered on No. 42 Whatman filter paper. The vanadium benzohydroxamic acid chelate was dried in a vacuum oven for 24 hours at 50°C. 65% yield was acheived with good purity. The melting point was found to be 150°C - 151°C by a Fisher-Johns melting point apparatus. 500 ml of a 0.1 M solution was made up in 1-Butanol (Mallinchrodt reagent grade lot BT C).

Instrument Operations:

Certain segments of this instrument require a warm up time. The oscilloscope needs at least one hour of warm up prior to use. The power oscillator has an external commercially available power supply associated with it. This is made by the Electronics Measurements Corp. in Eatontown, New Jersey and has 3 independently controlled voltage outputs. These include a 6.3 volt filament supply, a high voltage positive supply (V^+) and a low voltage negative supply (B^-). This enables the operator to keep the filaments powered without running the oscillator. This power should be on two hours prior to use. The Lavoie frequency meter should be connected

to 110 volt wall supply at least one week before using. It incorporates several calibrated crystal oscillators which are kept in ovens, the temperature of which must remain constant. The power should be on at least two hours before measurements are made. This instrument is used in conjunction with the low voltage output of the power oscillator, to determine which harmonic of the 500 KHz signal is being used.

Before measurements can be made, the parallelism of the crystals must be maximized. This procedure consists of placing the crystals, which are mounted on a drop plate, in distilled-deionized water and applying a signal. The output is displayed on the scope and is maximized by adjusting the spring loaded screws on the crystal mounts. This needs to be repeated only when the crystal mounting is somehow changed.

The sample container is now filled. The solvent (in this case 1-Butanol) is placed in the right compartment and the sample, (vanadium benzohydroxamic acid) is placed in the left. The crystals on the drop plate are moved over to the right so that the transmitting crystal is almost touching the membrane.

During this time, water from the constant temperature bath should be circulating through the water jacket of the cell. It may take several hours for the temperature to reach equilibrium. It is essential that drafts be avoided, as a $0.1^{\circ}C$ change in temperature can easily be seen in the form of signal strength fluctuation.

In preparation for engaging the R. F. pulse power oscillator, the operator must first check the double pulse generator which is shown in Figure 21. A 75 ohm coaxial cable is attached from the "sync" output of the double pulse generator to the external trigger input on the oscilloscope. The pulse output is examined on the 10 volt per cm scale. This pulse should be a 40 volt square wave. There is a three position pulse selector switch which chooses between the first pulse position that passes through the sample container, the second pulse position which passes through the attenuator network, and "operate" position, which is a combination of both. This is described in Figure 10. The width of both pulses, and the delay between the pulses can be adjusted by their respective controls on the front panel. Each control should be adjusted to be sure that the first pulse appears at the left of the scope and the second pulse appears to the right. This shows that the pulses and the oscilloscope are functioning properly. A cable connects the output of the double pulse generator to the input of the power oscillator. The power oscillator has a frequency range of 1 to 10 MHz. In order to get the selectivity, it was necessary to make both of the L. C. components of the circuit variable. Different coils have been wound on 3/4 inch plastic coil forms, which are of the "plug in" variety. After an appropriate coil is chosen, the V^+ supply can be applied. This is controlled by the electronics

FIGURE 21

A. A view of the double pulse oscillator

B. A view of the electronic measurements power supply

C. A view of the power oscillator

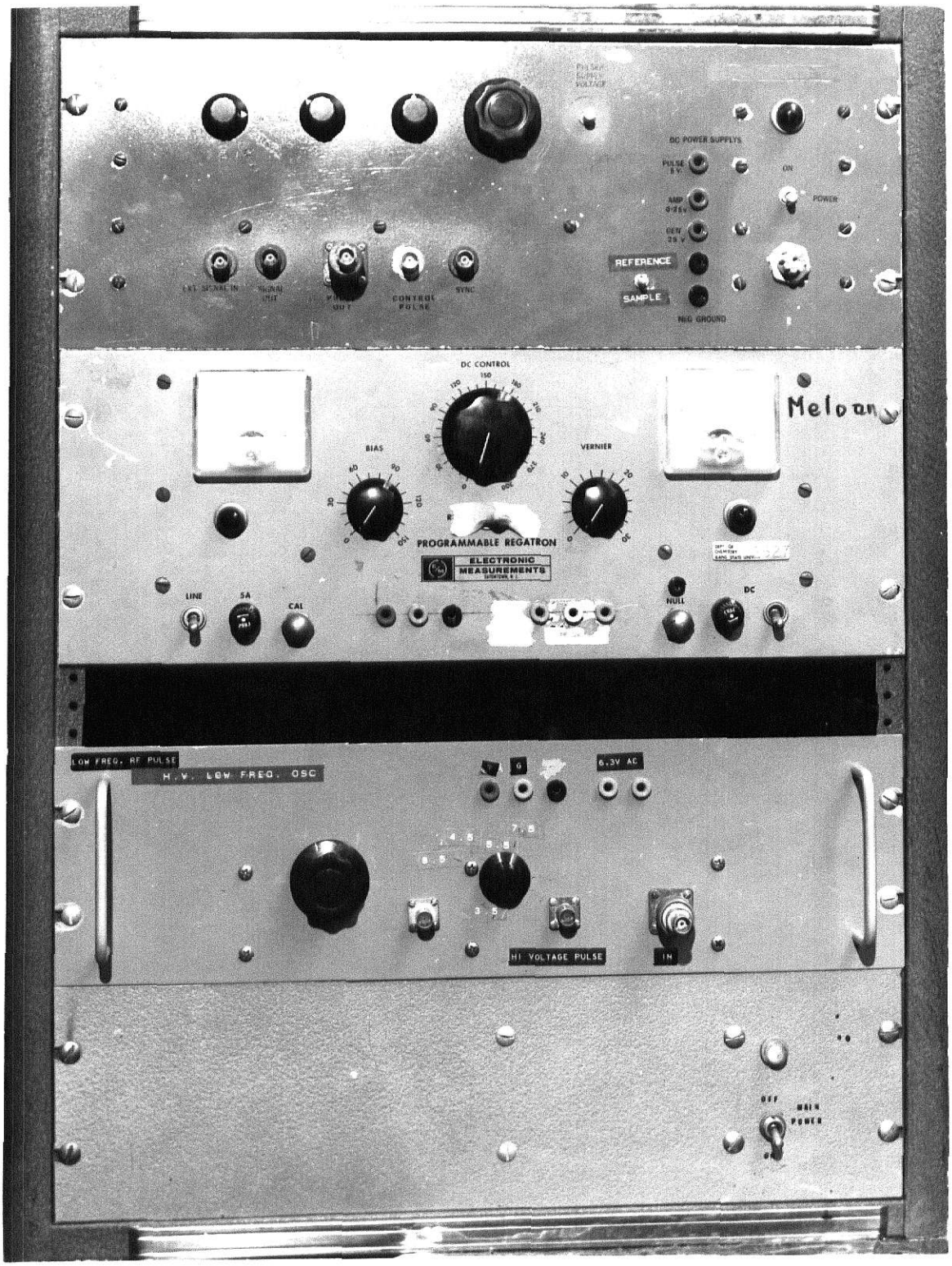
DC POWER SUPPLYS
PULSE 5 V.
AMP 0-25V
GEN 25 V
ON
POWER
REFERENCE
SAMPLE
NEG GROUND
EXT SIGNAL IN
SIGNAL OUT
CONTROL PULSE
SYNC
DC CONTROL
BIAS
VERNIER
PROGRAMMABLE REGATRON
ELECTRONIC MEASUREMENTS
LINE
5A
CAL
NULL
DC
LOW FREQ. RF PULSE
H.V. LOW FREQ. OSC
6.3V AC
HI VOLTAGE PULSE
IN
OFF
MAIN POWER

measurements power supply shown in Figure 21. The magnitude of this voltage will be adjusted to give the desired size R. F. pulse. It should be noted that since the crystals are a functional component of the circuit, they should be included by connecting a cable from the high voltage output to the crystals. This affects the loading of the oscillator and therefore should be done before any frequency measurements are made.

The low voltage output will serve double duty as a frequency measurement output and as the low voltage signal output which goes to the attenuator. The frequency of the pulse can be measured by either the oscilloscope or the frequency meter. Attaching the oscilloscope to this output, the R. F. pulses will be seen. The time base is then increased until the R. F. within the pulse can be seen as a true sine wave, which defends the treatment of the acoustic wave as being sinosoidal.

The frequency adjust control of the power oscillator varies the capacitor value in the L. C. tank circuit and will show a change in frequency on the oscilloscope as it is varied. It is then possible to determine the maximum and the minimum frequency for each coil. By knowing that only the odd harmonics of the crystals will be transmitted through the sample (i.e. 1.5, 2.5, 3.5, ... 9.5 MHz), the usable frequency of this coil can be determined. 18 coils were wound in all with different wire sizes and feedback ratios. A lot of

overlap occurred, and four coils were chosen which covered the entire spectrum of interest. With the type of L. C. network utilized here, the capacitor serves more as a trimmer than a tuner.

The low voltage output is tapped off the high voltage output and incorporates another variable capacitor. This variable capacitor serves as a magnitude control for the low voltage pulse and will come in very handy later for comparison purposes.

The receiver is now connected by attaching a cable from the receiving crystal of the cell to the cell input of the receiver. Another cable is connected from the attenuator network output to the attenuator input of the receiver. The low voltage output is connected to the input of the attenuator network and a cable connects the control pulse output of the double pulse generator to the control pulse input of the receiver. The oscilloscope is connected directly to the receiver, thus completing the system. A view of the receiver and the attenuator is shown in Figure 22.

Data Collection:

The power oscillator is adjusted to 1.5 MHz. The best way of assuring correct tuning is to watch the oscilloscope and tune until a deflection is observed. The oscilloscope now displays two peaks; the left peak corresponds to the sample and the right peak corresponds to the reference.

FIGURE 22

A. A view of the receiver

B. A view of the R. F. attenuation network

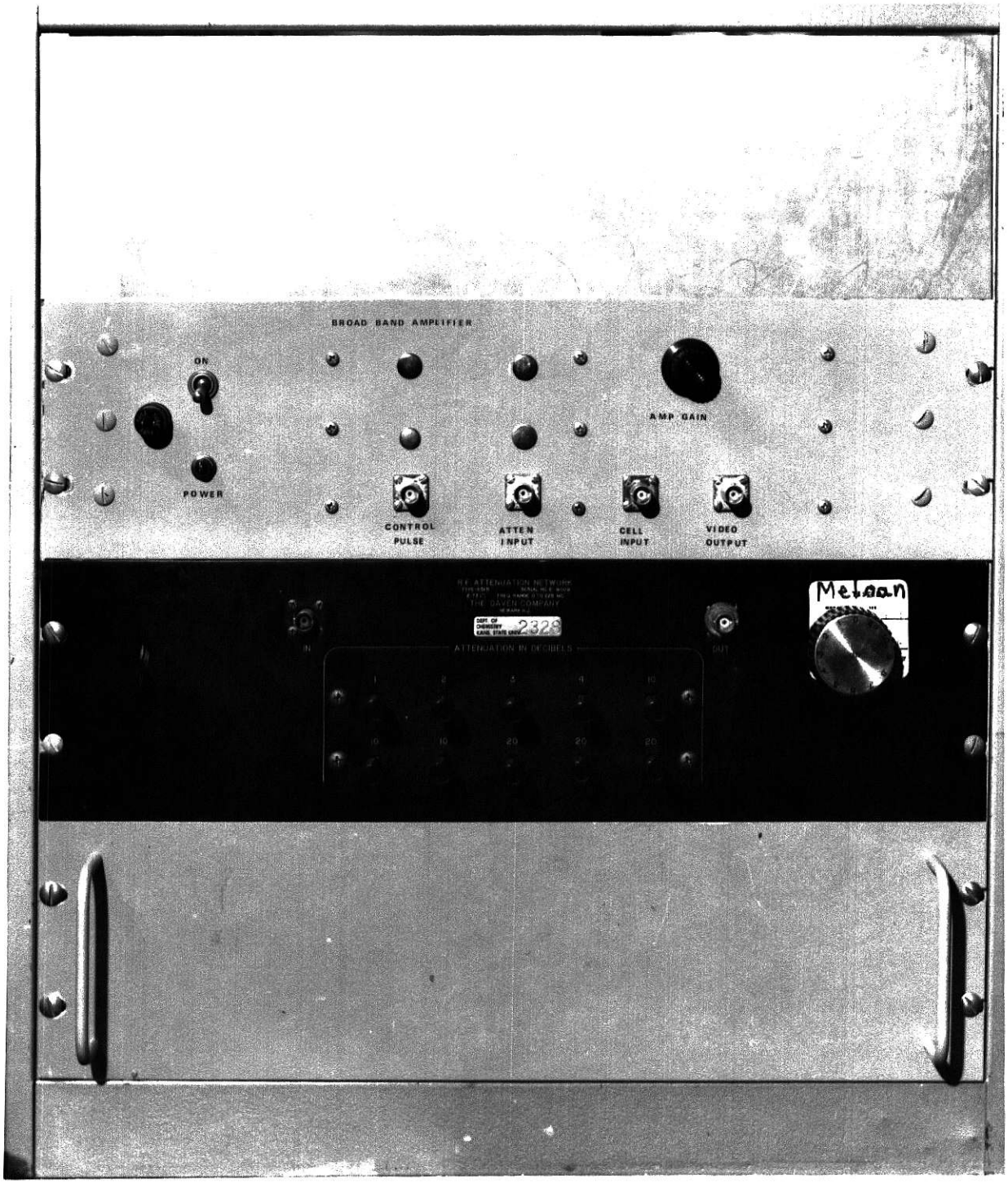
BROAD BAND AMPLIFIER
ON
POWER
AMP GAIN
CONTROL PULSE
ATTEN INPUT
CELL INPUT
VIDEO OUTPUT
THE DAVEN COMPANY
2328
IN
OUT
ATTENUATION IN DECIBELS
Melaan

The two peaks must be equalized, which is done by adjusting the tap off control on the power oscillator. If necessary, the attenuator network can be used to provide extra attenuation. In either case, the total amount of attenuation in db is noted. A change of 0.01 db is readily detected with the oscilloscope which is a factor of 10 more sensitive than needed. The attenuator network is then offset by some value. The amount of offset depends on the amount of absorption which will be encountered. This value can initially be set at 0.1 db and can be increased after the crystals move if needed. The reference peak should now show a decrease in height which corresponds to an attenuation of 0.1 db. The crystals are now moved to the left, thus decreasing the height of the sample peak. When the peaks become equal, the sample is said to have attenuated the signal by a 0.1 db. This amount of attenuation divided by the distance traveled, yields the absorption coefficient at 1.5 MHz. This should be repeated and should not vary more than 1 or 2 in the second decimal place. If deviations of larger than this occur, it is usually due to some outside variable which should be corrected. It is usually found that the discrepency is due to non-constancy of temperature.

When reproducible absorption coefficients at 1.5 MHz have been obtained, another frequency is selected and the absorption coefficient is determined at this frequency by the same process. This is done until an entire

spectrum of absorption coefficients are obtained at which time the data are fitted to the plot shown in Figure 1 and the relaxation frequency can be determined. This is done at several temperatures which, upon further analysis, yields equilibrium rate constants and the activation energy.

Results and Discussion

It was desired to obtain data at several temperatures to study the affect of temperature on the equilibrium rate constant, and ultimately determine the energy of activation. The temperatures studied in this work, are 22.7°C, 25°C and 30.5°C. Tables 1 and 2 show the data obtained at 22.7°C and 30.5°C respectively. Relaxation plots of these data are shown in Figure 23 and Figure 24, respectively. The relaxation frequency is obtained from the inflection point of these plots and the relaxation time is obtained via equation 24. The 25°C data was obtained from previous work and was used as a check set of data. Since relaxation processes are first order, the equilibrium rate constant can be calculated as simply the inverse of the relaxation time.

$$36) \quad \tau = \frac{1}{k}$$

where k is in units of sec^{-1}. Table 3 shows the kinetic parameters obtained in this work. The equilibrium rate constant is a function of the absolute temperature and is related to activation energy by:

$$37) \quad \frac{d \ln k}{d \left(\frac{1}{RT}\right)} = -E_a$$

TABLE 1

Absorption data at 22.7°C

Absorption data at 22.7°C

f (MHz)	α ($\times 10^3$ $\frac{db}{cm}$)	$\frac{\alpha}{f^2}$ ($\times 10^{16}$ $\frac{db-sec^2}{cm}$)	log f
2.5	0.938	1.50	6.39
3.5	4.24	3.46	6.54
4.5	3.33	1.65	6.65
5.5	6.65	2.19	6.74
6.5	7.16	1.70	6.81
7.5	6.63	1.18	6.88
8.5	8.50	1.18	6.93
9.5	10.26	1.14	6.98

TABLE 2

Absorption data at 30.5°C

Absorption data at 30.5°C

f (MHz)	α ($\times 10^3$ $\frac{db}{cm}$)	$\frac{\alpha}{f^2}$ ($\times 10^{16}$ $\frac{db\text{-}sec^2}{cm}$)	log f
2.5	1.30	2.08	6.39
3.5	4.43	3.60	6.54
4.5	6.45	3.19	6.65
5.5	7.55	2.50	6.74
6.5	1.42	3.35	6.81
7.5	1.89	3.36	6.88
8.5	2.30	3.18	6.93
9.5	1.16	1.27	6.98

FIGURE 23

Relaxation curve at 22.7°C

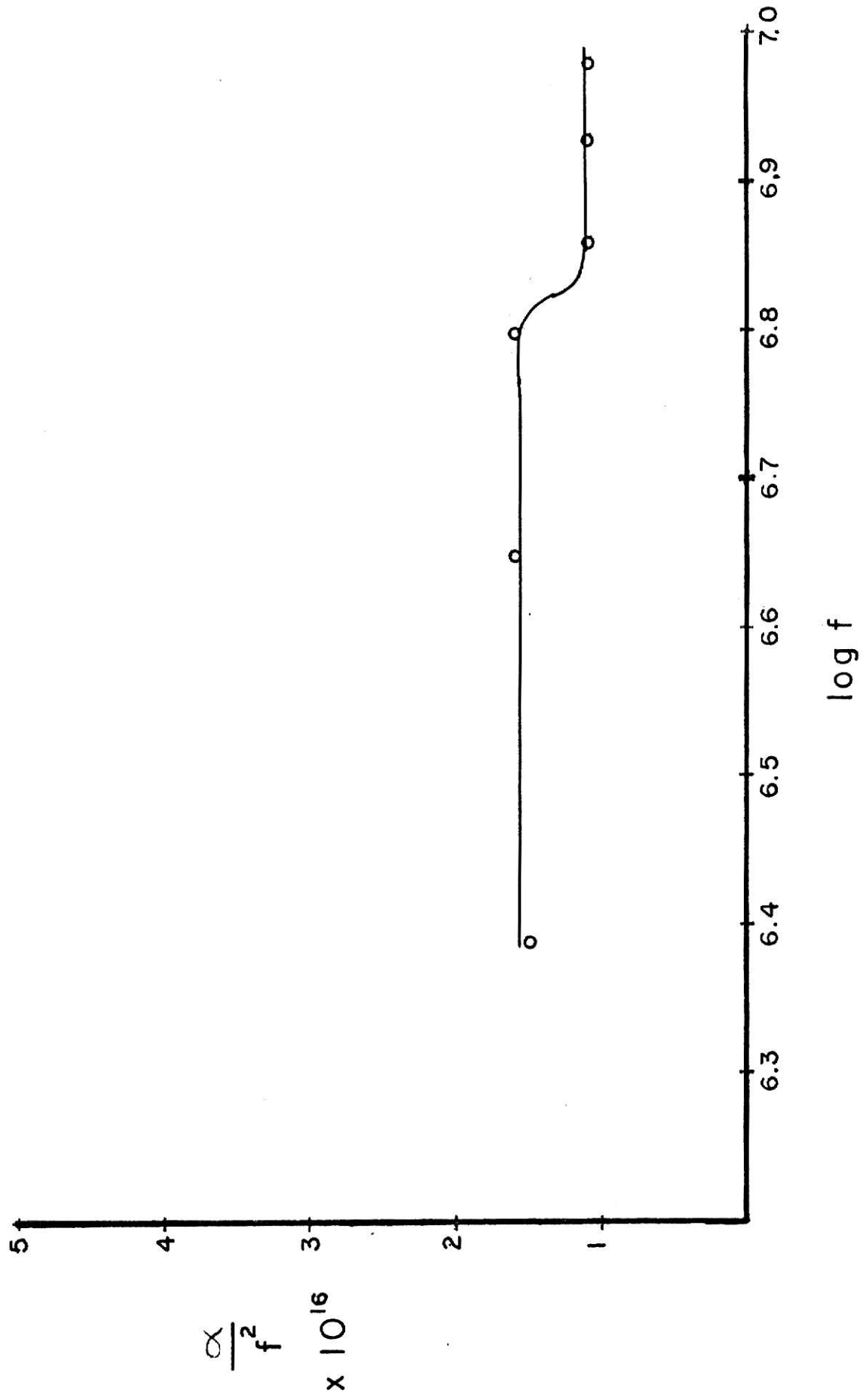
5
4
3
2
1
$\frac{\alpha}{f^2} \times 10^{16}$
6.3
6.4
6.5
6.6
6.7
6.8
6.9
7.0
log f

FIGURE 24

Relaxation curve at 30.5°C

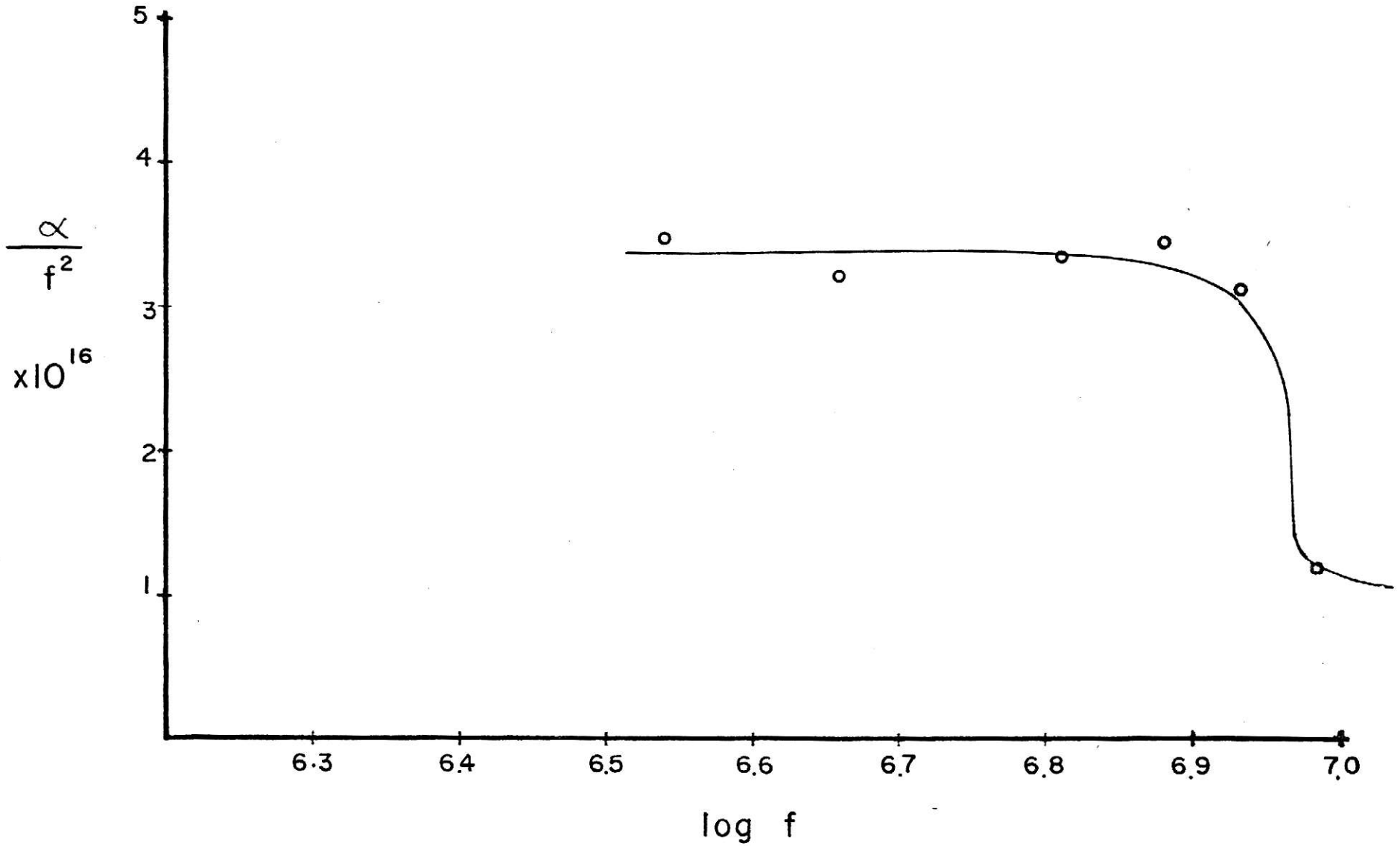
5
4
3
2
1
$\frac{\alpha}{f^2}$
x10^16
6.3
6.4
6.5
6.6
6.7
6.8
6.9
7.0
log f

TABLE 3

Kinetic parameters of vanadium benxohydroxamic acid.

Kinetic parameters of vanadium benzohydroxamic acid

fc (MHz)	τ ($\times 10^{8}$ sec)	k ($\times 10^{7} sec^{-1}$)	ln k	T (^{o}K)	$\frac{1}{T}$ ($\times 10^{3} K^{-1}$)
6.92	2.30	4.35	17.6	295.85	3.38
7.95	2.00	5.00	17.7	298.15	3.35
9.44	1.68	5.95	17.9	303.65	3.29

By intergrating this equation between the limits of $T = \infty$ to T, and rearranging to the form of the general equation $y = mx + b$, it is found that:

$$38) \quad \ln k_T = \frac{-E_a}{RT} + \ln k_\infty$$

A plot of this equation is shown in Figure 25. The activation energy is determined by the slope:

$$39) \quad M = \frac{-E_a}{R}$$

This value is found to be -6.6 Kcals $mole^{-1}$. k_∞ which is commonly called the pre-exponential factor is determined by extrapolating back to the y-axis and is found to be 3.44×10^{12} sec^{-1}.

Conclusion and Summary

The information obtained from this work describes the overall equilibrium conditions which exist between a metal chelate and the solvent adducts. The mechanism of this reaction was assumed to be a simple one step system. The possibility exists that a several step relaxation is occurring. To be able to predict the types of systems, further improvements are required on the instrumentation.

To detect the presence of a multi-step relaxation, the band width must be decreased and the frequency range must be increased. The band width could be narrowed by decreasing the harmonic of the ultrasonic transducer to 100 KHz. This alone would increase the resolution by a

FIGURE 25

A plot of ln k versus $\frac{1}{T^{o}K}$

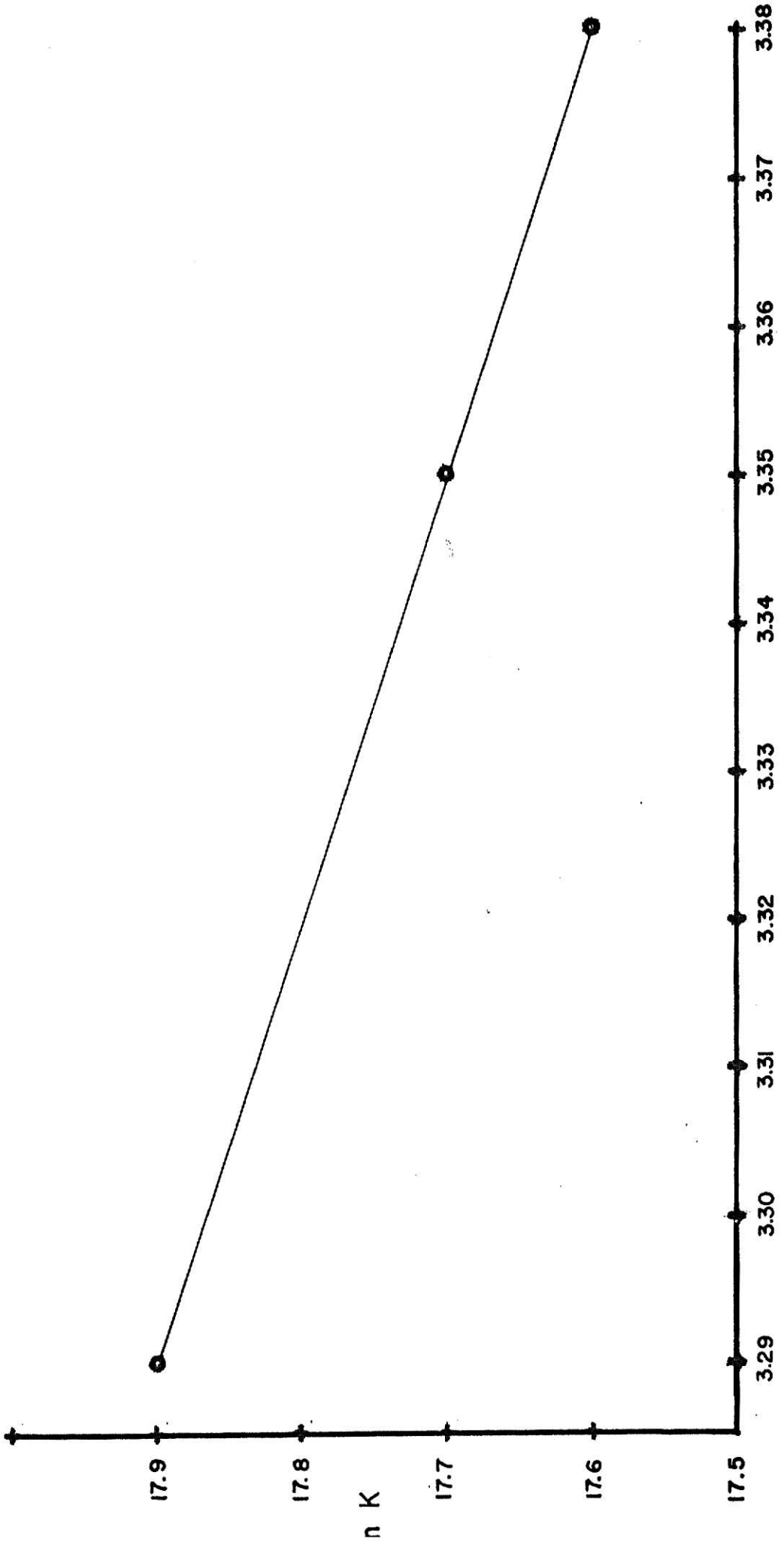
17.9
17.8
17.7
17.6
17.5
n K
3.29
3.30
3.31
3.32
3.33
3.34
3.35
3.36
3.37
3.38
$\frac{1}{T^{\circ}K} \times 10^3$

factor of 5. Next a more efficient transducer system would be needed so that the higher harmonics can be obtained without inducing prohibitive amounts of power. A possibility for this is the utilization of a push-pull transducer. This is made by sandwiching a resonant wedge between two crystals, and driving one crystal 180° out of phase with the other. This would literally push and pull the wedge back and forth in the solution. A diagram of a proposed model of this configuration is shown in Figure 26.

Assuming the above crystal configuration behaves as the author predicts, the driving signal does not need to be anywhere near the intensity at which we are now operating. This means that a low powered signal source can be used.

The signal source proposed could be a TTL logic oscillator which can easily deliver frequencies up to 100 MHz. Each harmonic could then be selected by choosing an appropriate divide-by counter. Three decades of thumbwheel switches could then select frequencies from 0.1 to 99.9 MHz. Ultimately a mini-computer could be used to scan these frequencies and store the signal output of the wide band receiver for each frequency. The crystals would then be moved a known distance and the frequencies would then be scanned again. The difference in signal intensity could now be determined immediately in terms of decibels per centimeter and the relaxation plots could be displayed on the terminal screen. This would be a true "Ultrasonic Spectrometer".

FIGURE 26

A proposed push-pull ultrasonic transducer

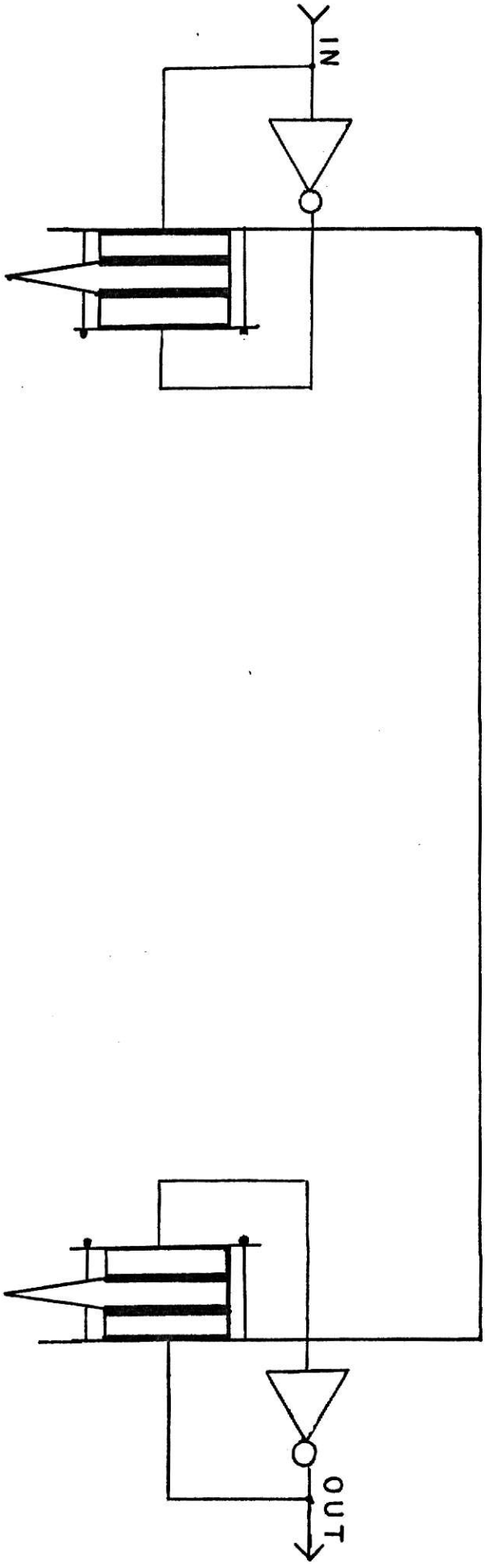
IN
OUT

This work has shown that the development of an instrument capable of determining a detailed description of the exchange rate between metal chelates and solvent adducts, is possible, and that such an instrument would become a useful analytical tool in studying extraction mechanisms.

BIBLIOGRAPHY

1. D.R. Gere and C.E. Meloan, J. Inorg. Nucl. Chem., 25, 117 (1963).

2. D.R. Gere and C.E. Meloan, Separation Sci., 3, 297 (1968).

3. D.R. Gere and C.E. Meloan, J. Inorg. Nucl. Chem., 25, 1507 (1963).

4. R. Motley and C.E. Meloan, Separation Sci., 3, 279 (1968).

5. R. Motley and C.E. Meloan, Separation Sci., 3, 285 (1968).

6. D.E. Noel and C.E. Meloan, Separation Sci., 7, 75 (1972).

7. J. Spigareli and C.E. Meloan, Separation Sci., 7, 85 (1972).

8. A.M. Ford, "An Instrument for the Measurement of Ultrasonic Attenuation", Part III Doctoral Dissertation, Kansas State University, Manhattan, Kansas 1972.

9. E.F. Caldin, "Fast Reactions in Solution," Blackwell Scientific Publication, Oxford (1964).

10. R.D. Corsaro, G. Atkinson and B.R. Perlis, Chemical Instrumentation, 2, 389 (1970).

11. "An Introduction to Piezoelectric Transducers," Valpey Corporation, Holliston, Mass., 1966.

12. "Digital Linear and MOS Data Catalog," Signetics, Sunnyvale, California, 1973.

13. "RCA Linear Integrated Circuit and MOS Devices," RCA Corp., Somerville, New Jersey, 1973.

14. "The Linear Integrated Circuits Data Catalog," Fairchild Semiconductor, Mountain View, California, 1972.

15. W.M. Wise and W.W. Brandt, Analyt. Chem., 27, 1392 (1955).

16. C.E. Meloan, M. Mauck and C. Huffman, Analyt. Chem., 33, 104 (1961).

ULTRASONIC ABSORPTION BY METAL CHELATES

by

JEFFREY BARTNER

B. S. College of Emporia, 1973

AN ABSTRACT OF A MASTER'S THESIS

submitted in partial fulfillment of the

requirements for the degree

MASTER OF SCIENCE

Department of Chemistry

KANSAS STATE UNIVERSITY

Manhattan, Kansas

1976

This thesis describes an instrument capable of measuring reaction rates of 10^6 sec^{-1} and faster. It employs a pulsed ultrasonic technique which perturbs the equilibrium of a metal chelate system and then measures the rate at which it returns to equilibrium. The chemical system studied was the formation of solvent adducts with the Vanadium (V) Benzohydroxamic acid chelate. Formation rates at various temperatures were obtained and the overall energy of activation was determined.

The perturbation of the equilibrium was induced by applying a pulsed radio frequency signal to a quartz crystal immersed in a sample. This transduces the R. F. wave to an acoustical pressure wave which alters the equilibrium conditions. The rate at which the equilibrium is re-attained can then be measured.

This instrument can be applied to aid in developing extraction mechanisms and improves the detection limits by a factor of ten over our previous instrument.